BRNO UNIVERSITY OF TECHNOLOGY
VYSOKÉ UČENÍ TECHNICKÉ V BRNĚ

FACULTY OF MECHANICAL ENGINEERING
FAKULTA STROJNÍHO INŽENÝRSTVÍ

INSTITUTE OF MATHEMATICS
ÚSTAV MATEMATIKY

DESIGN OPTIMIZATION OF PACKED BED FOR THERMAL ENERGY STORAGE
OPTIMALIZACE ZÁSOBNÍKU TEPLA TYPU "PACKED BED"

MASTER'S THESIS
DIPLOMOVÁ PRÁCE

AUTHOR — **Bc. Thomas Krist**
AUTOR PRÁCE

SUPERVISOR — **doc. Ing. Lubomír Klimeš, Ph.D.**
VEDOUCÍ PRÁCE

BRNO 2020

BRNO UNIVERSITY OF TECHNOLOGY
FACULTY OF MECHANICAL ENGINEERING

Specification Master's Thesis

Department:	Institute of Mathematics
Student:	**Bc. Thomas Krist**
Study programme:	Applied Sciences in Engineering
Study branch:	Mathematical Engineering
Supervisor:	**doc. Ing. Lubomír Klimeš, Ph.D.**
Academic year:	2019/20

Pursuant to Act no. 111/1998 concerning universities and the BUT study and examination rules, you have been assigned the following topic by the institute director Master's Thesis:

Design optimization of packed bed for thermal energy storage

Concise characteristic of the task:

A packed bed is a kind of the heat exchanger, which is applicable for thermal energy storage, often with air or water as the heat transfer fluid. A benefit of the backed bed is its suitability for various engineering applications with a wide range of the temperature. An optimal design of the packed bed is important for its effective operation.

Goals Master's Thesis:

The goal of the thesis is to create a computer simulation program for a packed bed. The type of accumulation particles will be chosen according to preferences of the student: for sensible heat thermal energy storage (e.g. rock particles) or for latent heat thermal energy storage (phase change material). A design optimization analysis by means of the created computer model will then be carried out.

Recommended bibliography:

MEHLING, Harald a CABEZA, Luisa F. Heat and cold storage with PCM: An up to date introduction into basics and applications. Heidelberg: Springer, 2008. ISBN 978-364-2088-070.

INCROPERA, Frank P., DEWITT, David P., BERGMAN, Theodore L. a LAVINE, Adrienne S. Principles of heat and mass transfer. Sedmé vydání. Singapore: John Wiley, 2013. ISBN 978-0-4-0-64615-1.

RAO, Singiresu S. Engineering optimization: Theory and practice. Čtvrté vydání. Hoboken: Wiley, 2009. ISBN 978-0-470-18352-6.

Deadline for submission Master's Thesis is given by the Schedule of the Academic year 2019/20

In Brno,

L. S.

prof. RNDr. Josef Šlapal, CSc. Director of the Institute	doc. Ing. Jaroslav Katolický, Ph.D. FME dean

Abstrakt
Tato diplomová práce se zabývá tématem výměny tepla v zásobníku tepla typu "packed bed". Cílem je popsat přenos tepla v zásobníku tepla obsahující kamínky malých průměrů, skrz který proudí horký vzduch. Toto je modelováno v prostředí MATLAB. Na začátku je krátký úvod do problematiky zahrnující ukládání tepla a jeho možné využití. Dále je uveden krátký přehled o základech přenosu tepla, typech přenosu tepla a termofyzikální vlastnosti systému vzduch-kámen. Ve třetí kapitole je představen zásobník tepla typu "packed bed" a rozličné modely a dané podmínky jsou vysvětleny. Další kapitola se zabývá s numerickými metodami, převážně s metodou konečných diferencí použitou v této práci. Pátá kapitola se zaměřuje na obecnou optimalizaci daného problému přenosu tepla. Populačně založený metaheuristický optimalizační algoritmus zvaný Genetický algoritmus je popsán. Sestavení modelu je ukázáno v šesté kapitole, stejně jako prezentace výsledků získaných z programu MATLAB. V poslední kapitole je pak diskutován závěr a doporučení.

Summary
This Master's thesis is dealing with the topic of heat exchange in a thermal energy storage unit of the type packed bed. The purpose is to describe heat transfer in a heat storage unit where hot air is flowing through that unit which is filled with stones of small diameter. This is designed in the environment of MATLAB. In the beginning, there is a brief introduction of the topic concerning heat storage and its possible use. Next, some short overview of heat transfer, types of heat transfers and thermophysical properties of the air-rock system are said. In the third chapter, the heat storage unit of type packed bed is introduced and various models and given conditions are explained. The next chapter is dealing with numerical methods, especially with the finite difference method used in this thesis. The fifth chapter is focusing on general optimization of the given heat transfer problem. A population-based metaheuristic optimization algorithm called the Genetic algorithm is described. The model setup is done in sixth chapter, as well as a presentation of results gained from MATLAB. In the last chapter, conclusions and suggestions are discussed.

Klíčová slova
ukládání tepla, zásobník tepla, packed bed, citelné teplo, tvarová optimalizace, genetický algoritmus, metoda konečných diferencí

Keywords
thermal energy storage, packed bed, sensible heat, design optimization, genetic algorithm, finite difference method

KRIST, T.*Design optimization of packed bed for thermal energy storage.* Brno: Vysoké učení technické v Brně, Fakulta strojního inženýrství, 2020. 83 s. Vedoucí doc. Ing. Lubomír Klimeš, Ph.D.

I declare that I have written the thesis "Design optimization of packed bed for thermal energy storage" on my own under the supervision of doc. Ing. Lubomír Klimeš, Ph.D. with the use of sources listed in the bibliography.

Bc. Thomas Krist

I would like to express my sincere gratitude to my supervisor doc. Ing. Lubomír Klimeš, Ph.D. for his useful comments and also for his guidance and patience throughout the creation of this thesis.

I would also like to thank to my parents for their love and support during my studies.

Bc. Thomas Krist

Contents

1 Introduction

With the progress in technologies, it is essential to use resources as effective as possible. Not only because of economical or technical reasons but also because of environmental reasons. With a growing population and a growing demand, the supply of energy, goods and services is growing as well. Often this happens on the expense of the environment. To satisfy both the growing demand and environmental friendly processes, newly invented technologies have to be used and optimized.

One of these environmental friendly technologies is the thermal energy storage (TES) process which uses a heat storage unit (HSU). This technology is depicted in Figure below. Heat can be saved in HSU in times of heat surplus and be used later, e.g. on a sunny day can the heat be collected from solar panels or from burning waste and in the night, it can be extracted to heat the flat/house or can be used to produce electricity. Two different ways of heat storage are known: sentive heat and latent heat. There are many kinds of HSU but in this thesis, only a HSU filled with particles will be assumed. This kind of HSU is called packed (or fixed) bed [17, 29].

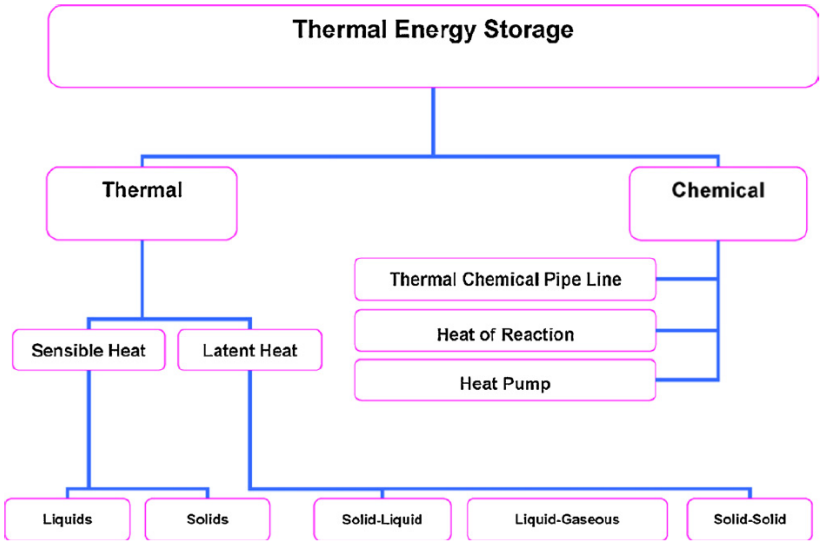

Figure 1.1: Various technologies of TES [29]

These packed beds (PB) have usually the shape of a vessel and are filled with particles of given shape and dimensions. In contrary to PB, there are also storage units called fluidized beds. As the names of both HSU suggest, in packed beds the particles are fixed, whereas in fluidized beds, the particles are not fixed and are in motion with the fluid flowing through the fluidized bed [1].

A good review of this topic was done by Harmeet Singh et al. [29] where various authors, which contributed to the study of heat transfer in packed, are mentioned. They also made a table where are listed authors which developed various correlations for Nusselt number Nu or heat transfer coefficient h_p.

Another good overview was done by J.A. Almendros-Ibáñez et al. [1]. Their work contains a comparison of packed and fluidized beds, as well as general information about heat storage using sensitive heat, latent heat and thermo-chemical energy storage.

2 Basics of heat transfer

This chapter deals with the basic laws and description of heat transfer such as conduction and convection. The section 2.1 is describing conduction and section 2.2 convection. For discussing heat transfer, it is also essential to know the properties used in thermomechanics. These properties are listed in section 2.3 and in 2.4 it is shown how these properties are changing with different temperature. In the last section of this chapter the partial differential equation used in this thesis is introduced and explained. For this chapter, the main sources will be [6, 11, 34].

Heat transfer, which is caused by a spatial temperature difference, is one of possible ways how to transfer energy from one system to another and is realized in the direction of decreasing temperature. In thermodynamics there are 3 different forms of heat transfer: conduction, convection and radiation.

Conduction is a heat transfer across a stationary medium (solid phase as well as fluid phase), in which there is a temperature gradient, whereas *convection* is a heat transfer between a surface and a non-stationary fluid of different temperatures. Surfaces of a finite temperature are emitting energy in the form of electromagnetic waves and this heat transfer is called *radiation*. Radiation will not be discussed, since it is not the aim of this Master's thesis to describe heat transfer via radiation.

The heat transfer can be expressed by parameters like *heat flux* (rate of heat transfer per unit area) $\dot{q}\,[\mathrm{W.m^{-2}}]$, and by *heat rate* $\dot{Q}$ [W]. The relation between heat flux and heat rate is given by the following equation:

$$\dot{Q} = \int_A \dot{q}\, dA = (T_\infty - T_s) \int_A h\, dA, \tag{2.1}$$

where A is the cross-sectional area perpendicular to the heat transfer and $\dot{q}$ is given by (2.5). If the heat transfer coefficient, and thus the heat flux, is not changing in the area A, i.e. it is constant, then according to [6] the equation (2.1) becomes:

$$\dot{Q} = \dot{q} \cdot A \tag{2.2}$$

2.1 Conduction

As it was explained in [6], due to Brownian motion, all molecules of a fluid are moving randomly (this random movement is also called *diffusion*), which causes that the molecules are interacting between each other, and thus the conduction can be understood as the heat transfer from particles with higher temperature to particles with lower temperature. Simply, heat conduction occurs, when there is no bulk motion in the fluid. On the other hand, the heat transfer in a solid is characterized by lattice waves, which are induces by atomic motion. To describe the heat transfer via conduction, the so called *Fourier's law* is used:

$$\dot{q} = -k\nabla T = -k\left(\mathbf{i}\frac{\partial T}{\partial x} + \mathbf{j}\frac{\partial T}{\partial y} + \mathbf{k}\frac{\partial T}{\partial z}\right), \tag{2.3}$$

where $\dot{q}$ is the heat flux and is perpendicular to the cross-sectional area A, ∇ is the 3-dimensional nabla operator, T is temperature and k is the thermal conductivity which is a characteristic of the material.

The equation (2.3) is given for a 3-dimensional space, but the model (3.5),(3.6) is just one-dimensional, so the Fourier's law is in the form:

$$\dot{q} = -k\frac{\partial T}{\partial x} \tag{2.4}$$

Further, conduction can be divided into 2 groups: *steady-state conduction* and *transient conduction*. The term steady-state means that the temperature in the system is independent of time, whilst transient means that the temperature is time-dependent [6].

2.2 Convection

Convective heat transfer occurs if, in addition to Brownian motion, there exist also a bulk motion. The term *convection* is used when referring to cumulative transport, and the term *advection* when referring to transport caused by bulk motion [6].

Convection depends on fluid properties such as dynamic viscosity, thermal conductivity, density of the fluid, specific heat and of course on the fluid velocity. Further it depends on the surface of the solid, i.e. on the geometry and on the surface roughness [11].

Convective heat transfer can be divided into forced convection and free (natural) convection. In the first case the flow of the fluid is forced by some external forces, i.e. a pump blowing hot air into a hollow cylinder or by wind. In the second case, the flow is induced by buoyancy forces, which are created by the differences in densities of the fluid (density differences are made by the temperature gradient). Heat transfer via convection can be described by the *Newton's law of cooling*:

$$\dot{q} = h(T_\infty - T_{ss}), \tag{2.5}$$

where h is the convection heat transfer coefficient, T_∞ is the temperature of the free fluid flow (temperature of the fluid before the heat exchange is realized), T_{ss} is the temperature of some solid surface. In (2.5) it is considered, that the heat transfer is positive to the surface (heat is transferred from the fluid to the surface), i.e. $T_\infty > T_{ss}$.

Further, the transferred heat can be divided into *sensible*, or internal heat, and *latent* heat. Sensible heat is the heat exchanged between two thermodynamic systems which changes the temperature of the systems. Latent heat is associated with a phase change of the system, usually solid to fluid phase change, in which the temperature during the phase change is constant. In this thesis, only sensible heat will be considered [6].

For simplicity, in this thesis it will be assumed that the solid particles, i.e. rocks, are perfect spheres and that the surface is smooth.

2.3 Thermophysical properties

In this section we will discuss the thermophysical properties, which are needed for the description of the heat transfer.

Thermal conductivity

The first thermophysical property is the thermal conductivity k, which gives us a rate of the ability to conduct heat in the material. In general, it varies with temperature, i.e. k has to be included in the derivatives, but for small-scale temperature variation, and thus for small value variations of k, the thermal conductivity can be considered to be constant at the *film (average) temperature*:

$$T_{film} = \frac{T_\infty + T_s}{2}. \tag{2.6}$$

That means, that k does not need to be included in derivatives.

The same procedure can be done also for other temperature-dependent properties, like specific heat or density [11].

The temperature of the solid surface is taken as the initial temperature of the solid phase $T_{ss} = T_s(x, 0) = 26.85\,^\circ\mathrm{C} \approx 27\,^\circ\mathrm{C}$ and the temperature of the free fluid flow will be the temperature of the dry air at the inlet, i.e. $T_\infty = T_f(0, t) = 126.85\,^\circ\mathrm{C} \approx 127\,^\circ\mathrm{C}$. Therefore, the film temperature $T_{film} = 77\,^\circ\mathrm{C} = 350$ K is obtained.

Heat transfer coefficient for particles h_p

It is the rate of heat transferred from the solid surface to the fluid per unit surface area and unit temperature difference. According to [11], when a no-slip condition is considered for a solid surface, the heat transfer coefficient from the surface to the fluid adjacent to the surface can be expressed by using thermal conductivity (since the heat is transferred by pure conduction). This is true in the case for a known temperature distribution in the fluid.

Before a proper formula of the heat transfer coefficient is given, some basic notions have to be introduced:

The *volumetric flow rate* (or also *volume velocity, rate of fluid flow*) is given by the fluid velocity v integrated over the whole area of interest A_{int}, i.e.

$$\dot{V} = \int_{A_{int}} v \, dA \tag{2.7}$$

Usually, the volumetric flow rate is denoted by Q but for clarity, $\dot{V}$ will be used. For a packed bed, the area of interest will be the void area A_{void} and thus

$$\dot{V} = \int_{A_{void}} v \, dA \tag{2.8}$$

In the case the packed bed (PB) is uniform (the particles in the PB have a cubic arrangement and not a random arrangement), the void area A_{void} is constant and can be expressed as

$$A_{void} = A \cdot \varepsilon \quad \Rightarrow \quad \dot{V} = v \cdot A_{void}, \tag{2.9}$$

where A is the cross-sectional area of the PB and ε is the void fraction of the PB [34].

Further it is important to introduce the *superficial velocity* (or also called *volumetrix flux*) v_{sv} which is a fraction of the volumetric flow rate and the cross-sectional area:

$$v_{sv} = \frac{\dot{V}}{A} = \left| \text{if } A_{void} \text{ is constant} \right| = \frac{v \cdot A_{void}}{A} = \frac{vA\,\varepsilon}{A} = v \cdot \varepsilon \tag{2.10}$$

The superficial velocity can be understood as the velocity over a given surface [34].

For the problem (3.7), (3.8), the temperature distribution is not known, so a correlation presented in [23] could be used:

$$h_v = 0.79 \cdot \left(\frac{G}{d_p} \right)^{0.7}, \tag{2.11}$$

where

$$G = \rho_f \, v_{sv} = \rho_f \, v \, \varepsilon$$

is the *superficial mass velocity* (or just *mass velocity, mass flux*), d_p is the diameter of the particle and h_v is the *volumetric heat transfer coefficient*. The unit of G is [kg/s·m^2] and the unit of the volumetric heat transfer coefficient is [W/m^3·K]. This correlation is using British Imperial Units, so to use it, the SI units have to be converted, inserted into (2.11) and the result has to be reconverted from British Imperial Units into SI units.

The formula (2.11) is used for convective heat transfer between the air and solid particles under the following conditions:

- range of inlet air temperature is 100 °F − 250 °F (37.8 °C − 121 ° C)
- superficial velocity has values between 12.05 ft/min and 66.3 ft/min (from 0.0612 to 0.3366 m/s)
- the size of particles is between 0.19" to 1.5" (0.48 cm – 3.8 cm)

In [23], it is also said that a reasonable extrapolation is justified.

The superficial mass velocity $G = 0.08$ kg/s·m^2 was obtained for the following given values:

- air velocity $v = 0.2$ m/s,
- void fraction $\varepsilon = 0.4$
- air density $\rho_f = 1$ kg/m^3
- and particle diameter $d_p = 1.6$ cm,

The air velocity was chosen freely and can be changed at will, but one should choose the air velocity such that the critical fluid velocity v_c is not exceeded (and therefore the fluid – gas can be considered as incompressible). The void fraction was computed in section 3.1. As for the particle diameter, this value was also chosen freely and can be changed at will but it has to be chosen so that the Biot number is less than 0.1 (and the intra-particle temperature gradient can be neglected).

To obtain the heat transfer coefficient for particles h_p, the following formula from [35] has to be used:

$$h_v = h_p \cdot \frac{6(1-\varepsilon)}{d_p}$$

This is one way of computing the heat transfer coefficient but another way of computing the heat transfer coefficient, which is described in section 3.4.1, will be utilized.

Heat transfer coefficient at wall h_w

To compute the temperature distribution in a PB, apart from using the heat transfer coefficient for particles h_p, it is also essential to know the heat transfer coefficient at the wall h_w [4]. As it was further said in [4], the heat transfer coefficient used for the particles is bigger than the one for the wall, due to different conditions. Thus, h_w can be considered as a constant multiple of h_p for a reasonable approximation. A multiple of 0.8, as suggested in [4], will be used:

$$h_w = 0.8\, h_p \tag{2.12}$$

Similarly to h_p, h_w will be also computed in section 3.4.1.

Specific heat

Using the information from [6, 11], the specific heat is the energy, which is needed to increase the material temperature of a unit mass by one degree. The specific heat can be distinguished between specific heat at constant pressure c_p and specific heat at constant volume c_v (here the subscript p stands for pressure and v for volume). It is known, that generally c_p is bigger than c_v. In general, specific heats are dependent on temperature and pressure, but for ideal gases, real gases at low pressure, and incompressible substances (solids and majority of liquids, they are dependent on temperature only. So for incompressible substances, it can be written $c_p \approx c_v$, and for ideal gases the following relations are used: $c_p = c_v + R$, $\gamma = c_p/c_v$, where R is the gas constant and γ is the heat capacity ratio or Poisson constant. The unit of the specific heat is [J/kg.K].

Dynamic viscosity

According to [11], viscosity of a fluid gives us the rate of resistance to flow and is dependent on temperature. For liquids, the viscosities are decreasing with temperature, and for

gases they are increasing. The viscosity can be divided into *dynamic viscosity* (also called *absolute viscosity*) μ and *kinematic viscosity* (or *momentum diffusivity*) ν. In [6] is the relation between both viscosities is given by the equation

$$\nu = \frac{\mu}{\rho_f}, \tag{2.13}$$

where ρ_f is the fluid density. The unit of dynamic viscosity is [kg/m·s] and of the kinematic viscosity is [m^2/s].

Thermal diffusivity

Thermal diffusivity is given by the following equation from [11]:

$$\alpha = \frac{k}{\rho c_p}, \tag{2.14}$$

where ρ is the density of the material and c_p is the specific heat at constant pressure. So thermal diffusivity represents how fast the heat is propagated trough the material. The unit is [m^2/s].

2.4 Dependence of thermophysical properties on the temperature

In this section, the dependence of thermophysical properties, such as density, thermal conductivity, etc. on the temperature will be discussed. Since the properties change with temperature, it is also important to consider at which temperature should be the properties evaluated. When dealing with a thermodynamical system, the properties can be calculated at:

- the average of highest and lowest temperature of the system
- the lowest temperature of the system
- the highest temperature of the system
- variable temperature (in our model we assume temperature-independent properties)

The most precise of these approaches is the one considering variable temperature, especially for high temperature operations ($\sim 400\,^\circ$C and more) [2]. In this thesis the temperature range of $27\,^\circ - 127\,^\circ$C will be considered.

As shown in [2] the temperature distribution for properties based on average (film) temperature are close, but not the same as for the case, where the properties are based on variable temperature. These differences will become more significant for higher temperature operations. So for a wide temperature range, it is important to consider temperature-dependent properties.

2.4.1 Properties of air

To determine the dependence of thermophysical properties on temperature, values from [32] has been taken (values of dry air at 1 atm):

Temperature T (K)	**Specific heat** $c_{p,f}$ (J/kg·K)	**Dynamic viscosity** μ (10^{-5} kg/m·s)	**Thermal conductivity** k_f (10^{-5} kW/m·K)	**Density** ρ_f (kg/m^3)
275	1003.8	1.725	2.428	1.284
300	1004.9	1.846	2.624	1.177
325	1006.3	1.962	2.816	1.086
350	1008.2	2.075	3.003	1.009
375	1010.6	2.181	3.186	0.9413
400	1013.5	2.286	3.365	0.8824
450	1020.6	2.485	3.710	0.7844
500	1029.5	2.670	4.041	0.7060
550	1039.8	2.849	4.357	0.6418
600	1051.1	3.017	4.661	0.5883
650	1062.9	3.178	4.954	0.5430
700	1075	3.332	5.236	0.5043
750	1087	3.482	5.509	0.4706

Table 2.1: Thermophysical properties of dry air [32]

So in Table 2.1, it can be seen, how the individual properties change with temperature for a range of 275 - 750 K. For a better overview, graphs 2.1 are shown below, using the data from Table 2.1. It should be noted that $c_{p,f}$ is specific heat at constant pressure for the fluid (subscript p stands for pressure and f for fluid).

For the specific heat of air, the values change from 1004 to 1087 J/kg·K, which is approximately 8.3 %. For our temperature range (300 - 400 K), it changes by 0.9 %. So the temperature dependence can be safely neglected without significant changes in the result. The value of dynamic viscosity at 750 K is twice as big as at 275 K, from 300 to 400 K, it changes by $\approx 24\%$. So here is a significant temperature dependence. Thermal conductivity changes by $\approx 127\%$ when considering the temperature up to 750 K, for 300 - 400 K, it is $\approx 28\%$. Density, on the other hand, does not increase with temperature, but decrease. It decreases by $\approx 63\%$ for the range 275 - 750 K, and by 25 % for the range 300 - 400 K. The thermal diffusivity is not shown in the table, but according to formula (2.14), α is dependent on specific heat, thermal conductivity and density, thus also thermal diffusivity will be dependent on temperature.

As it is seen, all properties, except specific heat, are significantly temperature dependent already by a temperature change of 100 K. But for simplicity of the model, these will be considered to be constant.

As already said, the temperature dependence is growing with increasing temperature, and for this, formulas suggested in [3] can be used for computing the thermophysical properties of air.

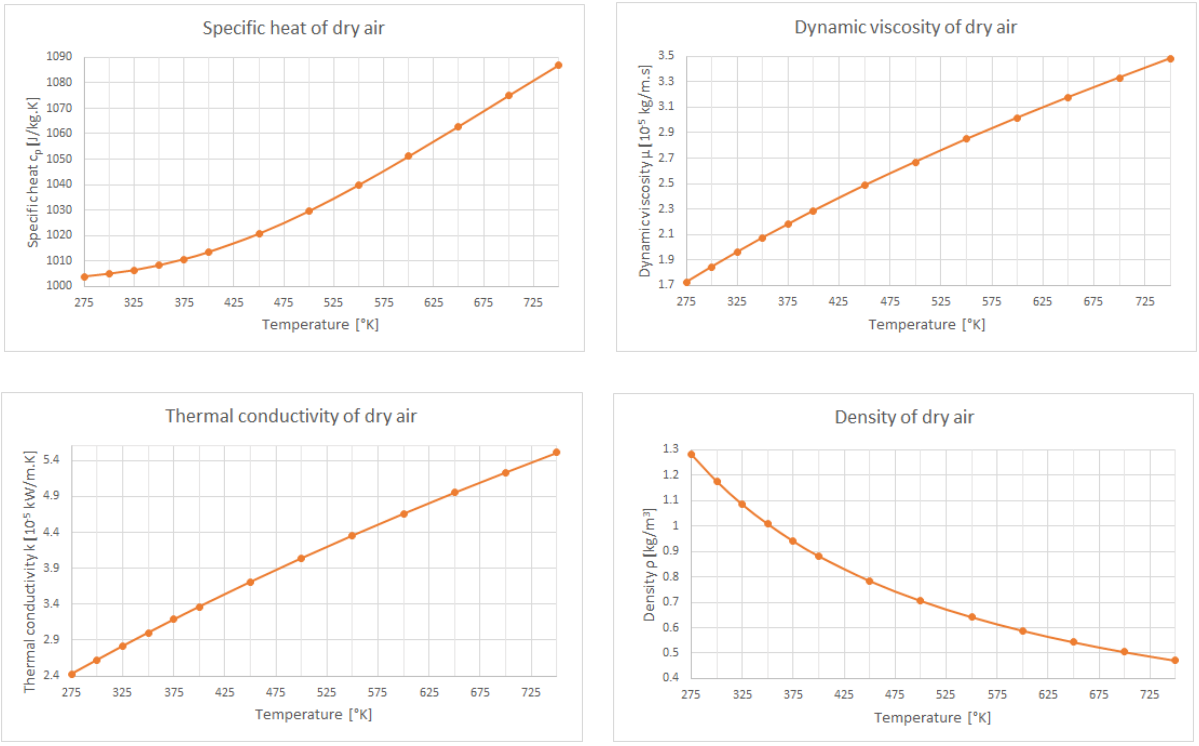

Figure 2.1: Thermophysical properties of dry air

So the thermophysical properties of dry air evaluated at the film temperature $T_{film} = 350$ K are as follows:

- specific heat $c_{p,f} = 1008$ J/kg·K
- dynamic viscosity $\mu = 2.075 \cdot 10^{-5}$ kg/m·s
- thermal conductivity $k_f = 0.03$ W/m·K
- density $\rho_f = 1.009$ kg/m^3 $\doteq$1 kg/m^3

2.4.2 Properties of rocks

Granite was chosen as the rock type, which could be possible used as heat storage material. The values are taken from [22].

As said in [22], the density at temperature of 500 °C was smaller by approximately 1 %, compared to density at room temperature, thus temperature dependence of density can be neglected. The density of granite rock is $\rho_s = 2550$ kg/m^3.

It was shown, that for the first heating cycle, heat capacity, thermal diffusivity and thermal conductivity are strongly dependent on temperature, but there is no permanent change for heat capacity, whereas for thermal diffusivity and thermal conductivity, after cooling down to room temperature, the values do not return to the initial ones. For subsequent heating and cooling cycles, no further permanent changes of properties occur, unless the previous temperature in the heating cycle is exceeded. This is called the *thermal*

Kaiser effect [22]. In other words, if the previous stress level is not exceeded during the present cyclic loading, no other crackings occur. These crackings need to be considered, since they irreversibly change the rock thermal properties [22].

Two groups of correlations have been developed - for initial heating and subsequent thermal cycles:

Initial heating:

$$c_{p,s} = 1.37 - 178 \cdot (T + 271)^{-1} \tag{2.15}$$

$$k_s = 2000 \cdot (T + 563)^{-1} \tag{2.16}$$

$$\alpha = 487 \cdot (T + 264)^{-1} \tag{2.17}$$

Subsequent heating/cooling:

$$c_{p,s} = 1.37 - 178 \cdot (T + 271)^{-1} \tag{2.18}$$

$$k_s = 3400 \cdot (T + 1385)^{-1} \tag{2.19}$$

$$\alpha = 526 \cdot (T + 400)^{-1}\,, \tag{2.20}$$

where T is the variable temperature in [° C], $c_{p,s}$ is the specific heat at constant pressure for solids (rocks) in [kJ/kg·K], α is the thermal diffusivity in [mm^2/s] and k_s is the thermal conductivity of the rocks in [W/m·K], and the correlations (2.15) – (2.20) are valid only up to 500 ° C. For higher temperatures, other correlations have to be used.

For designing of a PB with rocks as storage material, it has to be taken into account that a lot of thermal cycles will be realised, so both groups of correlations (2.15) – (2.17), (2.18) – (2.20) have to be used [22]. But for simplicity, only one heating phase will be considered in this thesis, i.e. the initial one.

For the correlations (2.15) – (2.17), the graphs 2.2 have been plotted:

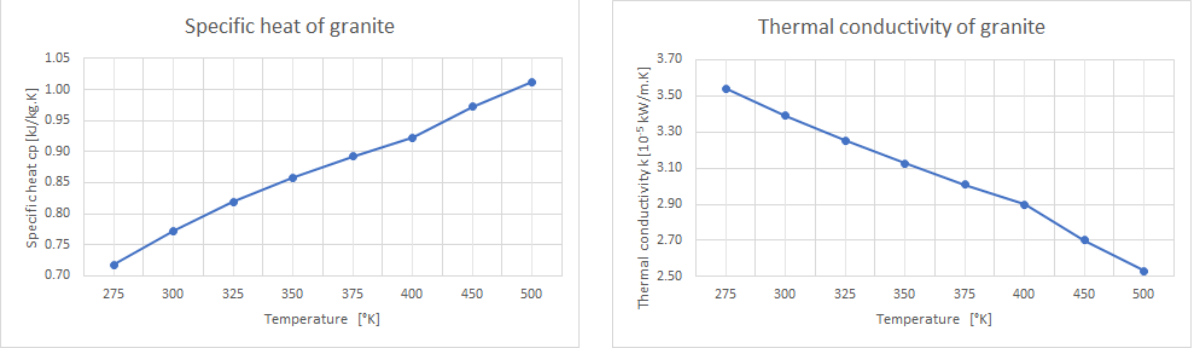

Figure 2.2a: Thermophysical properties of granite

Using the temperature range of 300 - 400 K the specific heat changes by 19 %, the thermal conductivity by 14.5 % and thermal diffusivity by 25.2 %. During the heating phase, only specific heat increases its value, conductivity and thermal diffusivity of granite in decreased. So the thermal properties of rocks are temperature dependent as well, but similarly as for air, they will be considered to be constant (same conclusion applies also for dimensionless numbers in section 3.4.1).

The conclusion is the same as for thermophysical properties of air, i.e. for big temperature changes, the correlations have to be used, otherwise inaccuracies will occur in the results.

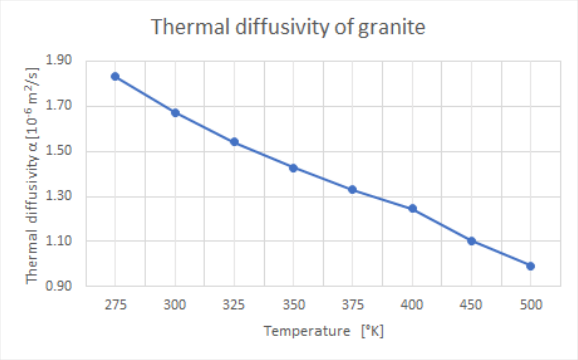

Figure 2.2b: Thermophysical properties of granite

For the computations, the thermophysical properties of granite evaluated at the film temperature $T_{film} = 350$ K will be used:

- specific heat $c_{p,s} = 859$ J/kg·K
- thermal conductivity $k_s = 3.125$ W/m·K
- density $\rho_s = 2550$ kg/m^3

2.5 Heat transfer using PDE

In this section, the use of partial differential equations (PDE) for heat transfer will be discussed. In the beginning, some basic notions are introduced. In section 2.5.1 are presented the basic boundary conditions used for PDE. The advection-diffusion-reaction equation is shown in section 2.5.2. The given equation is important for it will be used in chapter 3 to introduce the model used in this thesis. Therefore it is essential to know some basics about PDE since the heat transfer is following the principles of PDE.

First, some basic notion for PDEs will be introduced. A *Partial differential equation* of an unknown function $U(\xi_1, \xi_2, ..., \xi_n)$ has the form

$$F\left(\xi_1, \xi_2, ..., \xi_n, U, \frac{\partial U}{\partial \xi_i}, \frac{\partial^2 U}{\partial \xi_i^2}, ..., \frac{\partial^m U}{\partial \xi_i^m}\right) = 0, \tag{2.21}$$

where $\xi_1, \xi_2, ..., \xi_n$ are independent variables, $i = 1, 2, ..., n$. In other words, a PDE is an equation, where the partial derivatives of the unknown function U with respect to two or more independent variables are included [8, 26].

The *order* of a PDE is the highest derivative occurring in the equation, i.e. the number m. The equation is *linear*, if F contains only linear terms of the unknown function U and its derivatives, i.e. F does not contain terms with higher power than 1 (e.g. $U^2, \frac{\partial^3 U}{\partial \xi^3}, ..$), or products (for example $U_{\xi_1} \cdot U_{\xi_2}, U \cdot U_\xi, ...$). The equation is *homogeneous*, if it contains no constant terms, or terms which are not multiplied by U or its derivatives (for example $\xi_1, \xi_1^2, \xi_1 \cdot \xi_3, ...$) [26].

2.5.1 Initial and boundary conditions

For this section, the information will be obtained from [26].

To obtain a unique solution of the PDE, some initial and boundary conditions have to be prescribed. For simplicity, the following conditions will be written only for one spatial variable. The *initial condition* is given by

$$U(x, t_0) = U_0(x), \tag{2.22}$$

where t_0 is the initial time (usually $t_0 = 0$).

When the PDE contains only the first time derivative, one initial condition is needed. For a second order derivative, two initial condition are need. In other words, the number of initial conditions is given by the order of time derivatives contained in the PDE.

The *boundary condition* (BC) is prescribed at the boundary of the domain. The most common boundary conditions are the *Dirichlet BC*, *Neumann BC* and the *Robin BC*. The *Dirichlet BC* is given by

$$U(x, t) = f(x, t), \quad t > 0, \tag{2.23}$$

which can be understood as a prescribed temperature at the boundary.

The *Neumann BC* is given by

$$\partial_n U(x, t) = f(x, t), \quad t > 0, \tag{2.24}$$

where ∂_n is the normal derivative. This condition is describing, for example, the heat flux through the boundary

The last BC is the so-called *Robin condition*:

$$\alpha(x, t)\, \partial_n U(x, t) + U(x, t) = f(x, t) \tag{2.25}$$

2.5.2 Advection-diffusion-reaction equation

Consider a one-dimensional PDE in the following form:

$$U_t + v\, U_x = D U_{xx} - f(U) + S, \tag{2.26}$$

where D is the *diffusion coefficient* in the axial direction, v can be understood as *flow velocity*, *f(U)* is the *reaction*, which is a function of U, and S is the *source*. The equation (2.26) is called the *advection-diffusion-reaction equation* (or also *advection-diffusion equation with a reaction*). Sometimes, also the term *convection* is used instead of advection.

The abbreviation ADRE will be used for (2.26) [25]. This equation describes the evolution of some chemical species or substance in time and it can be derived from mass balances [20].

If $D = 0$, a *pure advection equation* is obtained. For $v = 0$, *the pure diffusion equation* is obtained and for $f(U) = 0$, an advection-diffusion equation is obtained. Further, if $S \neq 0$ then (2.26) is called *non-homogeneous*, otherwise it is *homogeneous* [10, 36, 28].

Usually is the ADRE non-linear and elliptic, so to find a solution is not a simple task, especially when convection is the dominating process. In the case of nonlinearities, the numerical stability for the standard finite difference method (SFDM) is in general not guaranteed, so other approaches have to be used, for example the nonstandard finite difference method (NFDM) [25].

3 Packed bed

This chapter is dealing with the thermal storage unit of the type packed bed. In the beginning, the construction of PB is explained. Afterwards, essential parameters for packed bed design like voidage are presented. Various models used for packed bed design and calculation are listed in section (3.2). From these models, only the continuous solid phase model has been used in this thesis to calculate the temperature distribution in the PB. This model is clarified in section (3.3). Further, dimensionless numbers (Reynolds, Prandtl number,...) and non-dimensional variables (non-dimensional time, temperature, etc.) are introduced and calculated in (3.4). These are used for numerical computations.

A packed bed (also called fixed or granular bed) is a hollow tube, vessel or a pipe, which is filled with particles (also called packing), and is used for food processing, chemical processing or heat storage (both low and high-temperature operations) [35].

The left picture in Figure 3.1 is showing the inner structure of a packed bed when cut horizontally. The packing is stored in the internal tube and the internal tube is covered by an insulation. On the right side is shown a vertical cut of a PB and inlet and outlet of gas.

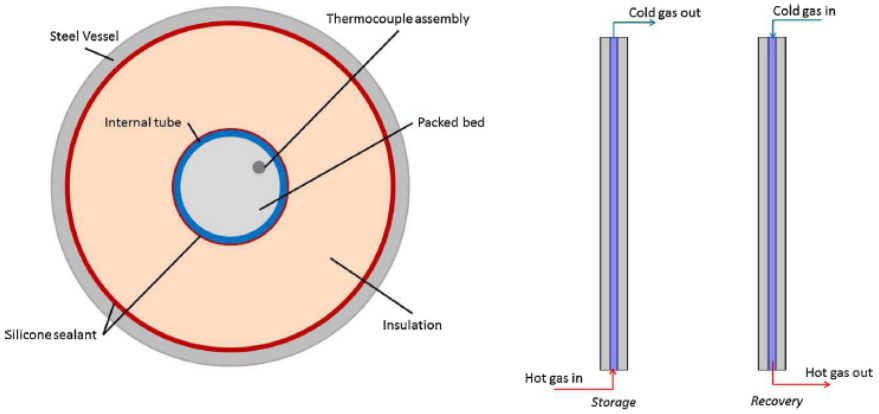

Figure 3.1: Packed bed [2]

According to [17] there are plenty of materials, which can be used for sensitive heat storage, like rocks, metals, concrete, sand, bricks and other. A good material is for example iron, since it has a good energy density level, but the disadvantage is the price, e.g. rocks and brick are less expensive so they are preferred as storage material.

Charging cycle of PB is done by hot fluid (which was heated i.e. by solar radiation) flowing through PB, where the fluid is heating up the storage material, and at the outlet the fluid is recirculated back to the solar panels to be heated up again. Naturally, the fluid at the outlet has a lower temperature during the charging cycle [2].

For the discharging cycle, the flow direction is reversed, so that fluid of a low temperature enters the PB and is heated by the storage material. The fluid has at the exit a higher temperature and can be used for some power cycle [2].

The stored energy depends on thermophysical properties of the storage material, but also on parameters like, particle size and shape, voidage (also called void fraction or porosity), heat transfer fluid (HTF), etc. [17].

Usually the combination of rocks as storage material and air as HTF heated by solar collector is used for temperatures around 100 °C, (but even up to 1000 °C) and particle sizes between 0.5 — 5 cm [17].

In Figure 3.2 a packed bed in a vertical cut is shown. From this picture the storage inside the internal tube is clear.

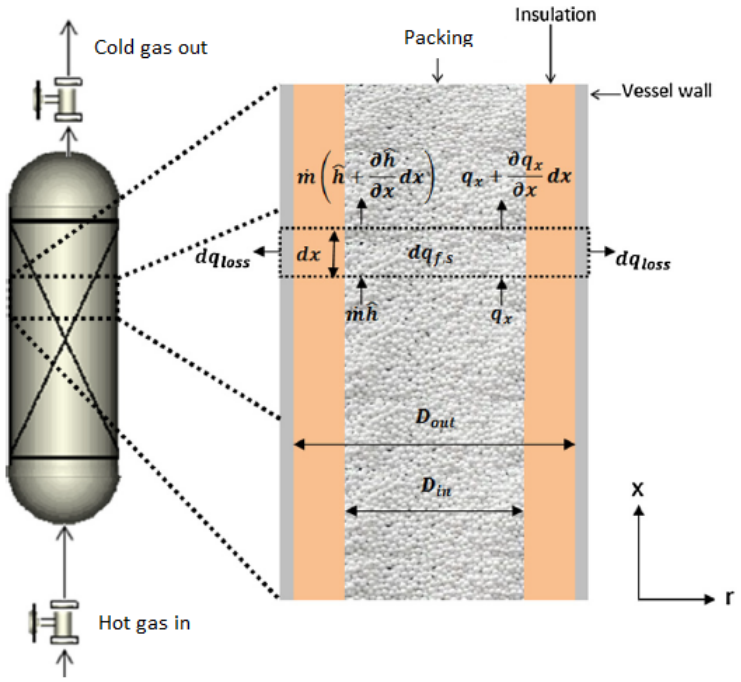

Figure 3.2: Structure of a packed bed [3]

As said in [35], main advantages of using air as working fluid and rocks as heat storage material are:

- common and economical material for heat storage
- big temperature range of usage, due to higher melting temperature of rocks
- no chemical instability
- no usage of chemicals or corrosive materials

In general, the particles can have many forms, i.e. beads (alumina beads were investigated in [3]), gravel [23], ellipsoidal shape [14], blocks or cylinders [31], etc. In Figure 3.3 are illustrated further possible particles.

TES systems must fulfill several condition for optimal heat storage:

- high energy density
- good heat transfer between the HTF (heat transfer fluid) and the storage material
- mechanical and chemical stability of the storage material
- low thermal losses to the ambient

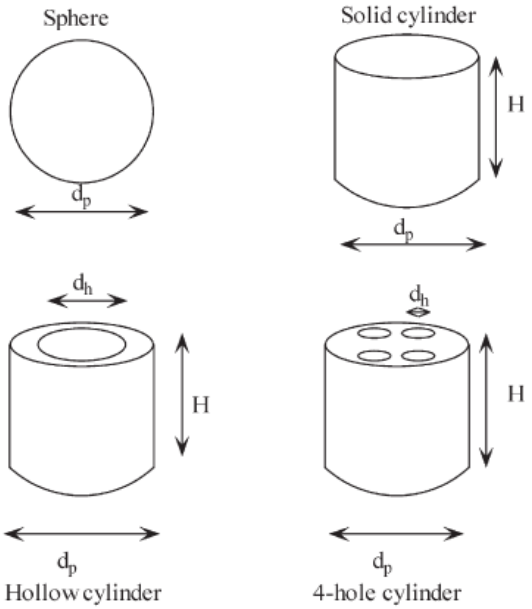

Figure 3.3: Possible particles as considered in [5]

- high number of reversible processes
- high exergy (measure of useful work in the system)

For PB to be efficient, there must be also a high degree of thermal stratification. Further, the fluid flow has to be considered such that the pressure drop is minimized, since a big pressure drop increases the destroyed exergy [2].

A detailed overview in designing PB is done in [29] where several authors are named and their contribution to the study of PB is shown.

3.1 Parameters

In this section, some parameters of PB will be discussed and computed, for example compressiblity, voidage and pressure drop.

The length of PB will be considered $L = 1$ m and the packed bed diameter $d_t = 0.2$ m.

Compressibility of the flow

To further analyse the flow in the PB, it has to be determined, whether the flow is compressible or incompressible. Flows with big density changes due to pressure drop are considered to be compressible. For liquids it can be assumed, that they are almost always incompressible, whereas for gases the density changes as the velocity approaches the speed of sound, i.e. the compressibility transition occurs at a critical Mach number $Ma_c \approx 0.3$.

Using *Mach number*

$$Ma = \frac{v}{a},$$

where

v is the gas velocity,
$a = \sqrt{\gamma RT}$ is the *speed of sound*,
$\gamma = c_{p,f}/c_{v,f}$ is the *ratio of specific heats of the fluid at constant pressure and constant volume*, respectively,
R is the *gas constant* and
T the temperature in Kelvins,
it can be computed for which gas velocities the flow needs to be considered as compressible, i.e. for $v > 0.3 \cdot a$ [6].

Considering that the the air velocity is $v = 0.2$ m/s and the air temperature $T =$ 350 K, the values of $c_{p,f}/c_{v,f}$ for dry air are obtained from [32]:

$c_{p,f}$= 1008.2 J/kg·K,
$c_{v,f}$ = 721.1 J/kg·K

From these values, γ and R can be computed (for R the formula from [6] will be used):

$\gamma = 1008.2/721.2 = 1.398$,
$R = c_{p,f} - c_{v,f} = 1008.2 - 721.1 = 287.1$ J/kg·K.

Now the speed of sound at $T = 350$ K can be computed (formula obtained from [6]):

$$a = \sqrt{\gamma RT} = \sqrt{1.398 \cdot 287.1 \cdot 350} = 374.8 \text{ m/s}$$

Multiplying the speed of sound by 0.3, the critical air velocity at 350 K is $v_c = 112.44$ m/s. So for air velocity of $v = 0.2$ m/s, the air flow can be considered as incompressible.

Voidage

According to [34] is the voidage a ratio of void volume of packed bed and total packed bed volume, i.e.

$$\varepsilon = \frac{V_{void}}{V_t} \tag{3.1}$$

Parameters, which increase the pressure drop, are the tube diameter and the particle diameter. With a bigger tube diameter, the pressure drop increases, whereas with a bigger particle diameter, the pressure drop decreases. For the model (3.7), (3.8), the following voidage correlation has been used:

$$\epsilon = 0.39 + \frac{1.74}{\left(\frac{d_t}{d_p} + 1.14\right)^2}. \tag{3.2}$$

The equation (3.2) is valid for $1.5 \leq d_t/d_p \leq 50$ [5].

So for particle diameter $d_p = 1.6$ cm $= 0.016$ m and diameter of the packed bed $d_t = 0.2$ m, we get the voidage $\varepsilon = 0.4$.

Pressure drop

As already mentioned, pressure drop increases the exergy destruction, thus the flow condition has to be considered to minimize the pressure drop [2]. The value of pressure drop is also essential for determining whether the fluid velocity, and thus the used fan power, is sufficient for a constant fluid circulation [6].

According to [13], the pressure drop is caused by losses in kinetic and viscous energy, where the total energy loss is the sum of kinetic and viscous energy losses. There are many factors that determine the pressure drop in PB, but the most important are: rate of fluid flow, fluid viscosity and density, closeness and orientation of particles (packing), the geometry and surface smoothness of the particles.

For a low flow rate, the pressure drop is proportional to the fluid (in our case gas) velocity, for higher flow rates the pressure drop is approximately second power of the fluid velocity. For the void fraction, the pressure drop is proportional to $(1-\varepsilon)^2/\varepsilon^3$ for low flow rates and $(1-\varepsilon)/\varepsilon^3$ for high flow rates [13].

To determine the pressure drop in the packed bed, the following equation from [13, 21] is used:

$$\frac{\Delta p}{L} = \frac{G^2}{\rho_f \, d_p} \cdot \frac{1-\varepsilon}{\varepsilon^3} \cdot \left(1.75 + 150 \cdot \frac{1-\varepsilon}{Re}\right) \tag{3.3}$$

where Δp is the pressure drop, L is the length of PB, G is the superficial mass velocity, ρ_f is density of the fluid phase, d_p is the particle diameter, ε is the void fraction and Re is the Reynolds number. the pressure drop was computed for the following values:

$G = 0.08$ kg/s·m^2,
$\rho_f = 1$ kg/m^3
$d_p = 1.6$ cm
$\varepsilon = 0.4$
$L = 1$ m
$Re = 61.6$ (Reynolds number will be computed in section 3.4.1)

The result is $\Delta p = 12.1$ Pa which is a small value, so the main conclusions are:

- the use of specific heat at constant pressure for dry air can be safely considered (instead of writing $c_{p,f}$ only c_f will be written)
- the exergy destruction is small
- no need to change any parameter to reduce the pressure drop.

Overall heat transfer coefficient for wall U_w

Another important parameter for PB modelling, is the overall heat transfer coefficient for wall and insulation which is taken from [21] and is defined by the following equation

$$U_w = \frac{1}{\frac{1}{A_t\, h_w} + \frac{ln\left(\frac{r_t + e}{r_t}\right)}{2\pi L k_{ins}} + \frac{1}{A_{ins}\, h_{ins}}}, \tag{3.4}$$

where A_t is the cross-sectional area of PB, h_w is the heat transfer coefficient at wall, L is the bed height, k_{ins} is the thermal conductivity of the insulation, r_t is the inner radius of the bed, e is the thickness of the insulation, A_{ins} is the cross-sectional area of the bed with insulation and h_{ins} is the heat transfer coefficient of the insulation to the ambient. To compute A_{ins} and h_{ins} the following equations are used:

$$A_{ins} = \pi \cdot (r_t + e)^2, \quad h_{ins} = 1.42 \left(\frac{\Delta T}{L}\right)^{\frac{1}{4}},$$

where $\Delta T = T_f - T_s = 100$ K. These equations are obtained from [21]. Considering the thermal conductivity of the insulation from [21] as $k_{ins} = 0.06$ W/m·K and $e = 0.25$ m, the following values are obtained:

$$h_{ins} = 4.49 \text{ W/m}^2\text{·K}, \quad A_{ins} = 0.385 \text{ m}^2, \quad U_w = 0.187 \text{ W/m}^2\text{·K}$$

3.2 Models

For heat transfer in fixed beds, 4 models were developed in the past, namely *Continuous solid phase model (CSPM), Schumann's model, Single phase model* and *Model with intra-particle temperature gradient* [21]. All models except the Single phase model are described by a system of two coupled partial differential equations, one for the solid phase (particles) and one for the fluid phase (gas – in our case air) [21].

The CSPM is considering both conduction and convection in both phase and both one-dimensional or two-dimensional approach can be used. The Schumann's model is derived from the one-dimensional case (radial direction is neglected) of the CSPM, but the axial conduction for both phases is not considered. In the third model, a thermal equilibrium is assumed between both phases. And for the last model, as the name indicates, a temperature gradient inside the particles is included [2, 21].

There are several assumptions for these models, i.e.

- the bed has a cylindrical geometry,
- the fluid and solid thermophysical properties are not dependent on the temperature,
- no heat is generated inside the bed,
- heat transfer via radiation is neglected (can be neglected only for low temperature operations),

- no chemical reactions occur inside the bed,
- for all models except the last, temperature gradients inside the particles are not considered,
- the packing is very small (this ensures uniform temperature inside the packing at any given time), except for the model with intra-particle temperature gradient,
- volume changes of packing due to rise of temperature are not considered,
- the flow of the fluid is uniform.

Further, also some losses to the ambient are considered [16, 21]. If any of these assumptions is not satisfied, additional terms have to be included in the model.

For a non-cylindrical tube, additional correlations for the Nusselt number, Reynolds number, etc. would have to be used [6]. The heat transfer by radiation can be neglected, since the majority of heat will be transferred by convection, and thus the radiation will have a small contribution to the heat transfer. But as shown in [35], for higher temperatures the radiation has a major contribution to the effective thermal conductivity, so it should be included for higher temperatures to obtain a more accurate solution.

The justification of the independence of thermophysical properties on the temperature has been done in section 2.4. As for the neglection of the temperature gradient inside the particles, the justification is done in section 3.4.1.

This thesis will deal only with the one-dimensional continuous solid phase model.

3.3 Continuous solid phase model

This section is using information from [21].

For this model it is assumed, that the filling (the particles) behaves like a continuous medium and not as single, independent particles. The two-dimensional heat transfer is given by the equations:

$$\begin{aligned}\varepsilon\rho_f c_f\left(\frac{\partial T_f}{\partial t}+v_\infty\frac{\partial T_f}{\partial x}\right) = k_{f,x}\frac{\partial^2 T_f}{\partial x^2}+k_{f,r}\left(\frac{\partial^2 T_f}{\partial r^2}+\frac{1}{r}\frac{\partial T_f}{\partial r}\right)+h_p a_p\left(T_s-T_f\right)\\ -U_w a_w\left(T_f-T_0\right)\end{aligned} \tag{3.5}$$

$$(1-\varepsilon)\rho_s c_s\frac{\partial T_s}{\partial t} = k_{s,x}\frac{\partial^2 T_s}{\partial x^2}+k_{s,r}\left(\frac{\partial^2 T_s}{\partial r^2}+\frac{1}{r}\frac{\partial T_s}{\partial r}\right)+h_p a_p\left(T_f-T_s\right), \tag{3.6}$$

where (3.5) is the equation for the fluid phase, and (3.6) the equation for the solid phase.

The left hand sides of Eqs. (3.5), (3.6) represent the rate change of enthalpy of the fluid and solid phase, respectively. In addition, in the first equation we have the net enthalpy associated with the fluid flow in the control volume. The first two terms on the right hand side of both equations represent the exchanged heat by conduction in axial and

radial direction, respectively. The third element in the equations is the heat exchanged by convection, and the last term in the first equation is the heat loss to the ambient.

As it was said in [21], to obtain the one-dimensional case of this model, the terms in radial direction need to be neglected:

$$\varepsilon\rho_f c_f \left(\frac{\partial T_f}{\partial t} + v_\infty \frac{\partial T_f}{\partial x} \right) = k_{f,x} \frac{\partial^2 T_f}{\partial x^2} + h_p a_p (T_s - T_f) - U_w a_w (T_f - T_0) \tag{3.7}$$

$$(1-\varepsilon)\rho_s c_s \frac{\partial T_s}{\partial t} = k_{s,x} \frac{\partial^2 T_s}{\partial x^2} + h_p a_p (T_f - T_s) \tag{3.8}$$

Since the equations (3.7), (3.7) are both in one dimension, it is not necessary to write the subscript x and so $k_{fx} = k_f$ and $k_{sx} = k_s$. Further, the multiplication of $h_p \cdot a_p$ and $U_w \cdot a_w$ is also called the volumetric heat transfer coefficient for the particles and overall volumetric heat transfer coefficient between the vessel (the packed bed) and ambient, respectively.

The model (3.5), (3.6) is clearly time-dependent, i.e. transient, since there is a time derivative in both equations. The same conclusion also hold for the one-dimensional model (3.7), (3.8).

3.3.1 Initial condition

The initial temperature is denoted by T_0 (for $t \leq 0$), and it is assumed that the initial temperature of the whole PB ($0 < x < L$) and of the fluid phase inside the PB are the same as the ambient temperature, i. e.

$$T_s(x,0) = T_f(x,0) = T_0 = 26.85\,^\circ\mathrm{C} \approx 27\,^\circ\mathrm{C}. \tag{3.9}$$

3.3.2 Boundary conditions

The boundary condition are taken the same as in [21]: outside of the PB, i.e. $x < 0$ and $x > L$, there is no heat exchange so the boundary conditions for solid phase are:

$$\frac{\partial T_s}{\partial x} = 0, \quad \text{for} \quad x = 0 \tag{3.10}$$

$$\frac{\partial T_s}{\partial x} = 0, \quad \text{for} \quad x = L. \tag{3.11}$$

For the fluid phase, the boundary conditions are similar, except at the inlet the fluid temperature is prescribed:

$$T_f = 127\,^\circ\mathrm{C}, \quad \text{for} \quad x = 0 \tag{3.12}$$

$$\frac{\partial T_f}{\partial x} = 0, \quad \text{for} \quad x = L. \tag{3.13}$$

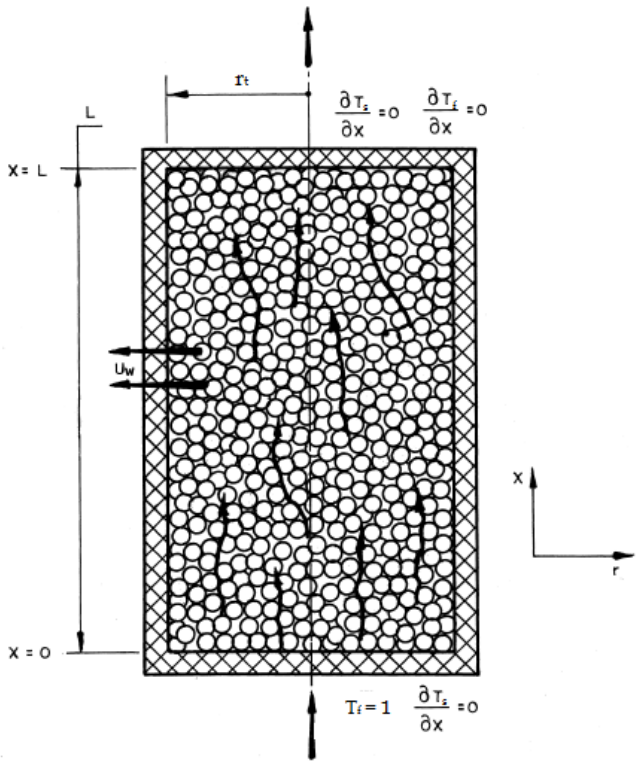

Figure 3.4: BC for the continuous solid phase model [21]

The boundary conditions are shown in Figure 3.4. This figure is not two-dimensional and it it can be clearly seen how the fluid flows through the packing.

Since this thesis will deal only with the one-dimensional version of the CSPM, the term "model" will refer to equations (3.7), (3.8) with initial and boundary conditions (3.9) – (3.13).

3.4 Non-dimensional parameters

The dimensionless numbers (also called similarity numbers) and non-dimensional parameters are essential in computation since the obtained dimensionless solution is not dependent on particular values of used temperature, heat transfer coefficient, thermal conductivity, length of PB, etc. This means that the dimensionless solution could be used for other problems where the values of parameters are different or the nature of the problem is different as long as the similarity number and the given geometry of both problems are the same. An example could be analogy of heat transfer and mass transfer in PB [6]. Another advantage of using non-dimensional parameters is a reduction of parameters used to describe the problem [11].

3.4.1 Dimensionless numbers

Reynolds number

The first similarity number is the Reynolds number, which is given by

$$Re_L = \frac{\rho V L_c}{\mu}, \tag{3.14}$$

and can be understood as the ratio of inertia and viscous forces with *characteristic dimension (characteristic length)* L_c. If Re_L acquires big values, then inertia forces dominate over viscous forces and vice-versa. Further the Reynolds number indicates, whether the flow is laminar or turbulent [6].

For the flow, 3 regions can be distinguished: laminar, transition and turbulent. In the laminar region the flow is ordered and the flow is called *laminar*. In the turbulent region the flow is not ordered, i.e. it is chaotic. The flow in the transition region is changing from laminar to turbulent and is characterized by the critical Reynolds number Re_c [6].

A formula from [21] has been used to obtain the Reynolds number:

$$Re = \frac{G\, d_p}{\mu}, \tag{3.15}$$

where G is the superficial mass velocity, d_p is the diameter of the particles and μ is the dynamic viscosity of air.

If the superficial mass velocity is $G = 0.08$ kg/s·m^2, $\mu = 2.075 \cdot 10^{-5}$ kg/m·s and $d_p = 1.6\,\text{cm} = 0.016$ m then the Reynolds number is $Re = 61.6$.

From [9], it is known that the transitional flow has Reynolds number of $2000 \leq Re_c \leq 4000$ and a fully turbulent flow has Reynolds number $Re > 5000$. Therefore, for the value $Re = 61.6$, the flow can be considered as laminar.

Prandtl number

The Prandtl number is given by the following equation:

$$Pr = \frac{c_f \cdot \mu}{k_f} = \frac{\nu}{\alpha}, \tag{3.16}$$

thus the Prandtl number is a ratio of kinematic viscosity (also called momentum diffusivity) ν, and the thermal diffusivity α. It gives us relative effectiveness of momentum and energy transport by diffusion in the velocity and thermal boundary layer. For $Pr \approx 1$ (for gases), the transfer of energy and momentum by diffusion are similar, for $Pr \ll 1$, the energy transfer is bigger than the momentum transfer by diffusion. In case $Pr \gg 1$, it is vice versa [6].

At the temperature 350 K, the dry air has following properties: $c_f = 1008$ J/kg·K, $\mu = 2.075 \cdot 10^{-5}$ kg/m·s, $k_f = 0.03$ W/m·K, and so the Prandtl number is $Pr = 0.6972$.

Biot number

The Biot number gives us a ratio of internal thermal resistance of solid to the boundary layer thermal resistance, in other words it gives us the amount of temperature drop inside the solid compared to the difference of surface and fluid temperatures, and is given by

$$Bi = \frac{h_p\, L_c}{k_s}, \tag{3.17}$$

where k_s is the thermal conductivity of the particles, h_p is the heat transfer coefficient for the particles and the characteristic length L_c is usually defined as $L_c = V/A$ and V, A are the volume and surface area of the given object. But in our case, i.e. for spheres, we will take $L_c = d_p$.

When $Bi \ll 1$ ($k_s \gg h$), then the heat is spread faster through the solid than through the interface fluid/solid, whilst if $Bi \gg 1$ ($k_s \ll h$), it is vice versa. This means that for $Bi \ll 1$ an uniform temperature inside the solid can be considered, i.e. no intra-particle temperature gradient occurs. Usually the condition $Bi < 0.1$ is used [6].

The Biot number will be computed after introducing Nusselt number.

Nusselt number

Nusselt number is the ratio of heat transfer modes: of convection to pure conduction. The equation is following:

$$Nu = \frac{h_p\, L_c}{k_f} = \frac{h_p\, d_p}{k_f}. \tag{3.18}$$

Again as with Biot number, if $Nu \ll 1$ ($k_f \gg h$), then the dominant heat transfer mode is conduction, whilst if $Nu \gg 1$ ($k_s \ll h$), then convection is dominant over conduction.

The difference between Nu and Bi is, that Bi is comparing thermal conductivity of the solid k_s to heat transfer coefficient h, and so it is used for solid, whilst Nu is comparing fluid thermal conductivity k_f to h, thus it is used for fluids [6].

As suggested in [34], the definition of Nusselt number for flow in PB is following:

$$Nu = \frac{h_p\, d_p}{k_f} \frac{\varepsilon}{1-\varepsilon}, \tag{3.19}$$

and another correlation stated in [4] could be used:

$$Nu = 2.42\, Re^{\frac{1}{3}} Pr^{\frac{1}{3}} + 0.129\, Re^{0.8} Pr^{0.4} + 1.4\, Re^{0.2} \tag{3.20}$$

Singh et al. [30] were conducting an experiment with the aim to obtain the Nusselt number also for non-spherical particles. They came with a correlation that is containing *sphericity* of the particle ψ. Sphericity is a parameter which is measuring how much the given object is similar to a sphere, i.e. for a sphere, the sphericity $\psi = 1$ and for a cube it is $\psi = 0.8$. The created correlation from [30] is following:

$$Nu_2 = 0.0614 \cdot Re^{1.1186} \varepsilon^{-1.0203} \psi^{2.5098} e^{(5.2979(ln\psi)^2)} \tag{3.21}$$

For a perfect sphere with $\psi = 1$, as it is in this case, the equation (3.21) has the following form:

$$Nu_2 = 0.0614 \cdot Re^{1.1186}\varepsilon^{-1.0203} \tag{3.22}$$

Wakao et al. [33] suggested another correlation for Nusselt number which is using only Prandtl and Reynolds number. The correlation is of the form

$$Nu_3 = 2 + 1.1Pr^{1/3}Re^{0.6} \tag{3.23}$$

The last correlation for Nusselt number will be taken from [15]

$$Nu_4 = 2.19Pr^{1/3}Re^{1/3} + 0.6Pr^{1/3}Re^{0.62} \tag{3.24}$$

Another way of computing h_p, h_w in section 2.3 could be by using the correlation of the Nusselt number (3.20) and by the use of (3.18), one could obtain the value of h_p. As it was said in section 2.3, h_w is smaller than h_p. This is expressed by the following equations:

$$h_w = 0.8\, h_p = 0.8 \left(\frac{k_f}{d_p} Nu\right) = 0.8\, \frac{k_f}{d_p} \left(2.42\, Re^{\frac{1}{3}} Pr^{\frac{1}{3}} + 0.129\, Re^{0.8} Pr^{0.4} + 1.4\, Re^{0.2}\right)$$

$$h_w = \frac{k_f}{d_p} \left(1.94\, Re^{\frac{1}{3}} Pr^{\frac{1}{3}} + 0.103\, Re^{0.8} Pr^{0.4} + 1.12\, Re^{0.2}\right) \tag{3.25}$$

Due to the reasons said in section 2.3, a second way of computing h_p and h_w will be used. The known values of Prandtl and Reynolds number will be inserted into (3.20) and the result $Nu = 14.68$ is obtained. For the second correlation in 3.22, the result is $Nu_2 = 15.68$. The result of the third correlation is $Nu_3 = 13.66$ and for the fourth it is $Nu_4 = 14.51$.

The next steps will be shown only with the correlation in (3.20) but the computation will be done with correlations in (3.20), (3.21). From (3.18), h_p will be computed:

$$h_p = \frac{Nu\ k_f}{d_p} = \frac{14.68 \cdot 0.03}{0.016} = 27.53\ \mathrm{W/m^2 \cdot K}$$

In the last step, h_w is computed:

$$h_w = 0.8\, h_p = 22.02\ \mathrm{W/m^2 \cdot K}$$

Knowing the value of h_p, the Biot number can be computed. For the values $h_p = 27.53$ W/m^2·K, $d_p = 0.016$ m and $k_s = 3.125$ W/m·K, the Biot number is $Bi = 0.141$ and so the condition for the neglection of intra-particle temperature gradient $Bi < 0.1$ is not satisfied but $Bi = 0.141$ is a low number, therefore $Bi << 1$, which is important.

Peclet number and effective thermal conductivity

The Peclet number is given by the equation

$$Pe = \frac{vL_c}{\alpha} = Re_L Pr, \tag{3.26}$$

where v is the fluid velocity, L_c is the characteristic dimension and α is the thermal diffusivity of the fluid. The Peclet number represents the ratio of heat transferred by advection to heat transferred by conduction [6]. Using the procedure from [21], for the model described in this thesis, the porous media has to be included, i.e. instead of flow velocity v the superficial velocity $v_{sv} = v\,\varepsilon$ is considered:

$$Pe = \frac{v_{sv}\,L}{\alpha} = \frac{v_{sv}\,\rho_f\,c_f L}{k_{ef,f}} = \frac{G\,c_f L}{k_{ef,f}}, \tag{3.27}$$

where $k_{ef,f}$ is the effective thermal conductivity of the fluid and according to [21] is computed as follows:

$$k_{ef,f} = \begin{cases} 0.7\;\varepsilon\;k_f & \text{if} \quad Re < 0.8 \\ 0.5\;Pr\;Re\;k_f & \text{if} \quad Re > 0.8 \end{cases}$$

Since the $Re = 61.6$, the second option for $k_{ef,f}$ has to be used and the value is $k_{ef,f} = 0.64$ W/m·K. From this, the Peclet number is $Pe = 125$.

To non-dimensionalize the equations (3.7), (3.8), the effective thermal conductivity of both fluid and solid phase will be used. This is important because as it was said in [21], heat transfer usually includes conduction, convection and radiation (radiation is not considered in this thesis). To include all the ways of heat transfer into a single parameter for fluid and one parameter for solid phase, the effective thermal conductivity has to be used. And because the effective conductivity for the fluid phase is already known, the computation of $k_{ef,s}$ is left. This will be done using the overall effective thermal conductivity as suggested in [21]. The overall effective conductivity k_{ef} is expressed as

$$k_{ef} = k_f \cdot \left(\frac{k_e^0}{k_f} + 0.5 Pr Re \right), \tag{3.28}$$

where $k_e^0 = k_f \cdot \left(\frac{k_s}{k_f}\right)^m$ for $m = 0.28 - 0.757 \log \varepsilon - 0.057 \log \left(\frac{k_s}{k_f}\right)$

The result is $k_{ef} = 1.46$ W/m·K and using the formula $k_{ef} = k_{ef,f} + k_{ef,s}$, $k_{ef,s}$ can be obtained. The value of $k_{ef,s}$ is 0.81 W/m·K.

3.4.2 Non-dimensional variables

In order to do the numerical computation, the equations and the initial and boundary conditions were non-dimensionalized using the formulas stated in [21], starting with non-dimensional coordinates:

$$x_d = \frac{x}{L}, \tag{3.29}$$

where x_d is the dimensionless axial coordinate, x the axial coordinate and L is the length of the PB. The following substitution was used for time:

$$\tau = \frac{G\, c_f\, t}{(1-\varepsilon)\rho_s\, c_s\, L}, \tag{3.30}$$

where G is the superficial mass velocity, c_f, c_s are the specific heats of fluid and solid phase, respectively, t is the actual time, ε is voidage of the PB, ρ_s is the solid density and L is the length of PB. If the total time is $t = 2\,\mathrm{h} = 7200\,\mathrm{s}$ then the dimensionless time is $\tau = 0.44$.

Another variable is λ which can be understood as the *ratio of volumetric thermal capacities of the fluid and solid phase* and is described by the following equation from [21]:

$$\lambda = \frac{\varepsilon\, \rho_f c_f}{(1-\varepsilon)\rho_s c_s} \tag{3.31}$$

For the given values from section 2.3, the ratio of volumetric thermal capacities is $\lambda = 3.06 \cdot 10^{-4}$.

As next, the Stanton number defined in [21] and [7] will be used. Usually is the Stanton number denoted as *St*, but in this thesis the notation from [21] will be used., i.e. Γ for particles and Γ_w for wall. These are described by the following formulas:

$$\Gamma = \frac{h_p a_p L}{G\, c_f} \tag{3.32}$$

$$\Gamma_w = \frac{U_w a_w L}{G\, c_f}, \tag{3.33}$$

where h_p is the heat transfer coefficients for particles, U_w is the overall heat transfer coefficient from the vessel to the ambient, a_p is the superficial particle area per unit bed volume [m^{-1}], a_w is the superficial area of the storage unit per unit volume of the bed [m^{-1}], G is the superficial mass velocity, c_f is the specific heat at constant pressure. To compute Γ, Γ_w, a_p and a_w will be needed and the equations from [34] will be utilized. The superficial area per unit bed volume of the particle (or also called particle surface area per unit volume) is computed by the following equation

$$a_p = \frac{A_p}{V_p} \cdot (1-\varepsilon), \tag{3.34}$$

where A_p is the surface of the particle and V_p is the particle volume. The result is $a_p = 225.24\ \mathrm{m}^{-1}$. The superficial area of the storage unit per unit bed volume is computed similarly:

$$a_w = \frac{A_t}{V_t} \cdot \varepsilon, \tag{3.35}$$

where A_t is the cross-sectional area of the PB and V_t is its volume [34]. So the value is $a_w = 0.4\ \mathrm{m}^{-1}$.

The computed values are $\Gamma = 77.02$, $\Gamma_w = 9.28 \cdot 10^{-4}$.

The following equations from [21] are used to convert the temperatures for fluid and solid phase, respectively:

$$T_{d,f} = \frac{T_f - T_0}{T_i - T_0} \tag{3.36}$$

$$T_{d,s} = \frac{T_s - T_0}{T_i - T_0}, \tag{3.37}$$

where $0 \leq T_{d,f} \leq 1,\ 0 \leq T_{d,s} \leq 1$ are dimensionless temperatures for the fluid and solid phase, respectively. For simplicity will the temperatures be denoted as follows: $T_{d,f}$ as T_1 and $T_{d,s}$ as T_2 [21].

By using (3.36), (3.37), the equations (3.7), (3.8) are obtained in the non-dimensional form:

$$\lambda \frac{\partial T_1}{\partial \tau} + \frac{\partial T_1}{\partial x} = \frac{1}{Pe} \frac{\partial^2 T_1}{\partial x^2} + \Gamma(T_2 - T_1) - \Gamma_w T_1 \tag{3.38}$$

$$\frac{\partial T_2}{\partial \tau} = \frac{k_{ef,s}}{Pe\, k_{ef,f}} \frac{\partial^2 T_2}{\partial x^2} + \Gamma(T_1 - T_2), \tag{3.39}$$

where $k_{ef,f}, k_{ef,s}$ are effective thermal conductivities of the fluid and solid phase, respectively, λ is the ratio of volumetric thermal capacities of the fluid and solid phase, Pe is the Péclet number and Γ, Γ_w are non-dimensional heat transfer coefficients [21].

When the equation (3.38) is divided by λ, it can be seen, that both (3.38), (3.39) are advection-diffusion-reaction equations with a source term on the right-hand side, i.e. with terms $\frac{\Gamma T_2}{\lambda}$ in (3.38), and with ΓT_1 in (3.39).

Since the solid temperature is expressed in the equation for the fluid phase and vice-versa, both temperatures are interacting with each other, and these equations are said to be *coupled* [36].

All properties were assumed to be temperature independent, and therefore all coefficients in (3.38), (3.39) are constant and need not to be included in the derivatives. Furthermore are both equations linear, which is simplifying the procedure to obtain the solution.

3.4.3 Non-dimensional initial and boundary conditions

Using equations (3.36) and (3.37), the non-dimensional initial temperatures of the solid and fluid phase are obtained:

$$T_1(x, \tau) = T_2(x, \tau) = 0, \qquad \text{for } \tau \leq 0, \quad 0 < x < 1, \tag{3.40}$$

and the non-dimensional boundary conditions for solid and fluid phase (for $\tau > 0$) are respectively:

$$\left.\frac{\partial T_2(x,\tau)}{\partial x}\right|_{x=0} = \left.\frac{\partial T_2(x,\tau)}{\partial x}\right|_{x=1} = 0 \tag{3.41}$$

$$T_1(0, \tau) = 1, \quad \left.\frac{\partial T_1(x,\tau)}{\partial x}\right|_{x=1} = 0 \tag{3.42}$$

The boundary conditions (3.41) and the seccond condition in (3.42) are saying that there is no heat flux (no heat is exchanged) at the inlet and outlet of the packed bed. As for the first conditions in (3.42), this is the non-dimensional form of (3.12), saying that the fluid temperature at the inlet is maximal, i.e. $127\,^{\circ}\mathrm{C}$. The initial conditions (3.40) are saying, that both phases are at the room temperature, i.e. $\approx 27\,^{\circ}\mathrm{C}$ [21].

4 Numerical methods and implementation of the model of a packed bed

In this chapter, the use of numerical methods for solving the heat transfer by PDE will be shown and explained. First, some basic requirements and definitions which will be necessary for a discussion of applicability of the chosen numerical method are stated. In the section (4.1) the finite difference method (FDM) along with the stability analysis is presented and explained. This method will be used for the numerical computation. As a suitable program was chosen MATLAB.

Often the PDEs do not have an analytic (or exact) solution, so by an appropriate numerical method, an approximate solution of the PDEs can be found [10]. For an analytic solution we can determine the temperature in any point, whereas for a numerical (approximated) solution we can determine the temperature only in discrete points (due to discretisation) [6].

According to [36], for using a numerical method, a few requirements have to be acknowledged:

- accuracy of the used method
- convergence of the approximate solution to the exact solution of the differential equation
- consistency
- stability of the numerical method
- efficiency of the method

For a numerical solution to converge to the exact solution, stability and consistency of the used scheme is needed, which is illustrated by the following scheme from [20]:

$$\textit{stability} \ \& \ \textit{consistency} \Rightarrow \textit{convergence}$$

Further some important notions have to be introduced:

Definition 1. The *point-wise error* is $e_i^n = u_i^n - U_i^n$, where u_i^n is the approximate solution at the point (x_i, t_n) and U_i^n is the exact (analytical) solution at the point (x_i, t_n) The point-wise error is also called the *global error* or *round-off error* [10, 19].

Definition 2. The *truncation error* at the point x_i and at the time t_n is defined as $D_{\Delta t, \Delta x} U_i^n$, where U_i^n is the exact solution and $D_{\Delta t, \Delta x}$ is the difference operator, i.e. the operator which defines the used finite difference scheme. This error is also referred to as *dicretization error* since it is dependent on the used discretization method and its mesh [10, 19].

The accuracy of a numerical method is given by the truncation error, which is a measure of inaccuracy, when a continuous variable is approximated by discrete points (or how well does the finite difference scheme satisfy the exact solution). The truncation error depends on the spatial step size Δx, so with more points discretizing the continuous variable, i.e. with a finer mesh, a smaller truncation error is obtained, and thus a better accuracy of the used method. So a scheme with a small truncation error has to be used [8, 10, 36].

According to [10, 36], for consistency of the approximate scheme and the differential equation, it is important that the approximation is identical to the differential equation in the limit, as the mesh size is decreasing to zero. In other words, the truncation error goes to zero as the steps $\Delta x, \Delta t$ decrease to zero:

$$D_{\Delta t, \Delta x} U_i^n \to 0 \tag{4.1}$$

The scheme is stable, if the error is bounded with increasing time, i.e.:

$$|e^{n+1}| \leq |e^n|, \tag{4.2}$$

where $n \geq N$ is the time level [10, 36].

As it was already said, for convergence of a finite difference scheme, a scheme which is stable and consistent is needed.

For a scheme to be efficient, it is essential to consider a compromise between the accuracy and the time consumption, since with a better accuracy the time consumption is increasing [36].

4.1 Finite difference method

For using the finite difference method (FDM), the region of interest has to be replaced by a finite grid, also known as *mesh*. Further the distance between two spatial nodes is denoted by Δx, and Δt the distance between two time nodes. Both distances are calculated by these formulas:

$$\Delta x = \frac{L}{N-1} \qquad \Delta t = \frac{t_f}{M-1}, \tag{4.3}$$

where N is the desired number of spatial nodes, M is the desired number of time nodes and t_f is the final time [10].

So the region of interest (in our case the PB of the length L) is replaced as following:

$$\begin{aligned} x_1 &= 0 \\ x_2 &= x_1 + \Delta x \\ &\vdots \\ x_i &= x_{i-1} + \Delta x = x_1 + (i-1)\Delta x \\ &\vdots \\ x_N &= x_{N-1} + \Delta x = L \end{aligned} \tag{4.4}$$

The finite difference method is based on Taylor's expansion, where the derivatives are replaced by polynomials, thus the derivatives are approximated by adjacent values using the Taylor's theorem.

Consider the equation (2.26). The theorem says, that if the value of U and the value of derivatives of U at the point x_i are known then the value at the point x_{i+1} can be obtained, where $x_{i+h} = x_i + \Delta x$ [10].

The following FD schemes will be applied for derivatives in (3.38), (3.39):

$$\frac{\partial T}{\partial \tau} = T_\tau(x_i, \tau_n) \approx \frac{T_i^{n+1} - T_i^n}{\Delta \tau} \tag{4.5}$$

$$\frac{\partial T}{\partial x} = T_x(x_i, \tau_n) \approx \frac{T_i^n - T_{i-1}^n}{\Delta x} \tag{4.6}$$

$$\frac{\partial^2 T}{\partial x^2} = T_{xx}(x_i, \tau_n) \approx \frac{T_{i+1}^n - 2\,T_i^n + T_{i-1}^n}{(\Delta x)^2} \tag{4.7}$$

The approximation (4.5) is called the forward time difference, (4.6) the backward spatial and (4.7) the symmetric spatial difference. This scheme is of first order in time and in space. These differences are illustrated in Figure 4.1 [10].

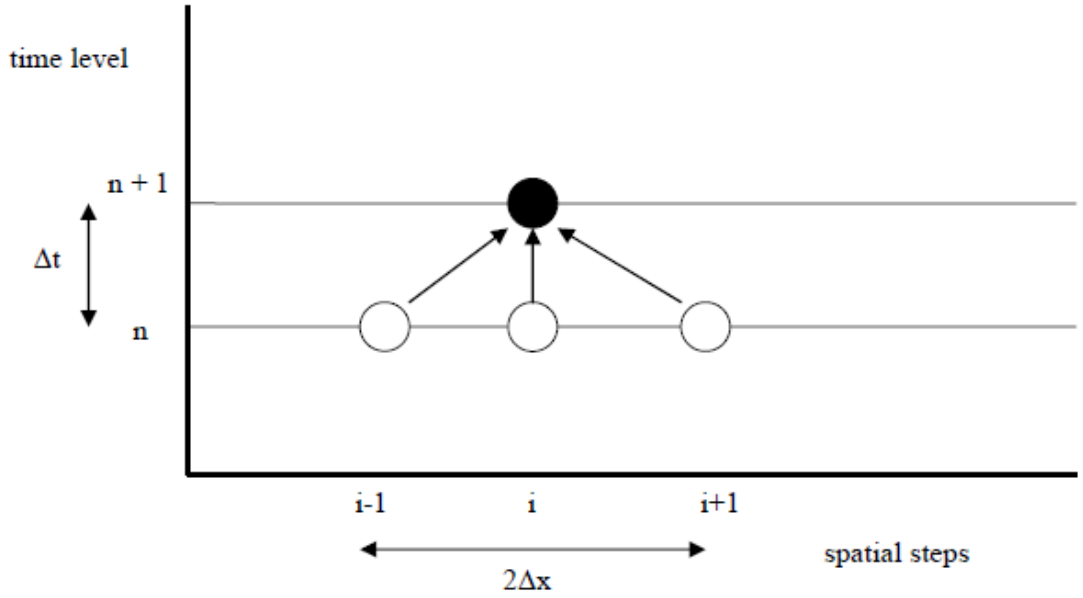

Figure 4.1: Forward time centered space approximation [10]

Since an explicit finite difference scheme is used, some restrictions on the time step Δt need to be applied, so that the approximation converges to the exact solution (stability criterion is generally described in section 4.1.3) [10].

When substituting (4.5) – (4.7) into the model (3.38), (3.39), the following is obtained:

$$\begin{aligned} T_{1,i}^{n+1} = {} & T_{1,i+1}^{n}\left(\frac{\Delta\tau}{Pe\,\Delta x^2\,\lambda}\right) + T_{1,i}^{n}\left(1 - \frac{\Delta\tau}{\Delta x\,\lambda} - 2\frac{\Delta\tau}{Pe\,\Delta x^2\,\lambda} - \frac{\Delta\tau(\Gamma+\Gamma_w)}{\lambda}\right) \\ & + T_{1,i-1}^{n}\left(\frac{\Delta\tau}{\Delta x\,\lambda} + \frac{\Delta\tau}{Pe\,\Delta x^2\,\lambda}\right) + T_{2,i}^{n}\frac{\Gamma\Delta\tau}{\lambda} \end{aligned} \tag{4.8}$$

$$\begin{aligned} T_{2,i}^{n+1} = {} & T_{2,i+1}^{n}\left(\frac{\Delta\tau\,k_{ef,s}}{Pe\,\Delta x^2\,k_{ef,f}}\right) + T_{2,i}^{n}\left(1 - \Gamma\Delta\tau - 2\frac{\Delta\tau\,k_{ef,s}}{Pe\,\Delta x^2\,k_{ef,f}}\right) \\ & + T_{2,i-1}^{n}\frac{\Delta\tau\,k_{ef,s}}{\Delta x^2\,Pe\,k_{ef,f}} + T_{1,i}^{n}\,\Gamma\Delta\tau, \end{aligned} \tag{4.9}$$

where the first bracket on the right-hand side of (4.8) is denoted as A, second as B and the third as C. Similarly for (4.9), i.e. first bracket on right-hand side as D, second as E and the third as F. So (4.8), (4.9) can be rewritten as:

$$T_{1,i}^{n+1} = A\,T_{1,i+1}^{n} + B\,T_{1,i}^{n} + C\,T_{1,i-1}^{n} + T_{2,i}^{n}\frac{\Gamma\Delta\tau}{\lambda} \tag{4.10}$$

$$T_{2,i}^{n+1} = D\,T_{2,i+1}^{n} + E\,T_{2,i}^{n} + F\,T_{2,i-1}^{n} + T_{1,i}^{n}\,\Gamma\Delta\tau, \tag{4.11}$$

where $i = 1, ..., N$ is the *i-th* spatial node, and $n = 1, ..., M$ is the *n-th* time node.

The equation (4.10) can be also described using matrices as following:

$$\begin{pmatrix} T_{1,1}^{n+1} \\ \vdots \\ T_{1,N}^{n+1} \end{pmatrix} = \begin{pmatrix} B & A & & & & \\ C & B & A & & & \\ & C & B & A & & \\ & & \ddots & \ddots & \ddots & \\ & & & C & B & A \\ & & & & C & B \end{pmatrix} \begin{pmatrix} T_{1,1}^{n} \\ \vdots \\ T_{1,N}^{n} \end{pmatrix} + \frac{\Gamma\,\Delta\,t}{\lambda} \begin{pmatrix} T_{2,1}^{n} \\ \vdots \\ T_{2,N}^{n} \end{pmatrix} \tag{4.12}$$

The same can be done also for (4.11):

$$\begin{pmatrix} T_{2,1}^{n+1} \\ \vdots \\ T_{2,N}^{n+1} \end{pmatrix} = \begin{pmatrix} E & D & & & & \\ F & E & D & & & \\ & F & E & D & & \\ & & \ddots & \ddots & \ddots & \\ & & & F & E & D \\ & & & & F & E \end{pmatrix} \begin{pmatrix} T_{2,1}^{n} \\ \vdots \\ T_{2,N}^{n} \end{pmatrix} + \Gamma\,\Delta \begin{pmatrix} T_{1,1}^{n} \\ \vdots \\ T_{1,N}^{n} \end{pmatrix} \tag{4.13}$$

The first matrices on the right hand side in (4.12) and (4.13) are tridiagonal matrices. These matrices would be important for the stability analysis but as it will be explained in the next sentences and in section 4.1.2, these matrices were not used for stability analysis.

After considering the implementation of this procedure, it was decided that it would be easier to do only discretization for the spatial derivatives, i.e. for terms

$$\frac{\partial T_1}{\partial x}, \frac{\partial^2 T_1}{\partial x^2}, \frac{\partial^2 T_2}{\partial x^2},$$

instead of also for the time derivatives. The main reason for this was that the equations (4.10), (4.11) were too difficult for obtaining the stability condition and it would be better to let MATLAB decide what the size of the time step will be.

After the partial discretization, the equations (4.10), (4.11) became

$$\dot{T}_{1,i} = A\,T^n_{1,i+1} + B\,T^n_{1,i} + C\,T^n_{1,i-1} + \frac{\Gamma}{\lambda}\,T^n_{2,i}, \quad i = 2, ..., N \tag{4.14}$$

$$\dot{T}_{2,i} = D\,T^n_{2,i+1} + E\,T^n_{2,i} + F\,T^n_{2,i-1} + \Gamma\,T^n_{1,i}, \quad i = 1, ..., N \tag{4.15}$$

The terms A, B, C, D, E, F are as follows:

$$A = \frac{1}{Pe\,\Delta x^2\,\lambda}$$
$$B = -\frac{1}{\Delta x\,\lambda} - \frac{2}{Pe\,\Delta x^2\,\lambda} - \frac{\Gamma + \Gamma_w}{\lambda}$$
$$C = \frac{1}{\Delta x\,\lambda} + \frac{1}{Pe\,\Delta x^2\,\lambda}$$
$$D = \frac{k_{ef,s}}{Pe\,\Delta x^2\,k_{ef,f}}$$
$$E = -\Gamma - \frac{2\,k_{ef,s}}{Pe\,\Delta x^2\,k_{ef,f}}$$
$$F = \frac{k_{ef,s}}{\Delta x^2\,Pe\,k_{ef,f}}$$

The equations (4.14), (4.15) were changed into matrix form and the created matrix was used to create the code in MATLAB.

4.1.1 Boundary conditions

To solve a PDE by finite difference method, ghost points at the beginning or at the end have to be specified, depending on the used scheme. This is described in Figure 4.2 where the black points are grid points and the white one is the ghost point [10].

Since the spatial differences are (4.6), (4.7), both left and right ghost points will be needed (except for temperature T_1 at the inlet of PB, i.e. for point $i = 1$, since the left BC of T_1 is saying that fluid temperature will be at any time the maximal one and therefore there is no need to compute the temperature at the inlet), i.e. together with point $i = 0$ also the point $i = N + 1$ is needed.

The boundary conditions (3.41), (3.42), except the first condition in (3.41), are all *Neumann boundary conditions* which specify the rate of change of the dependent variable

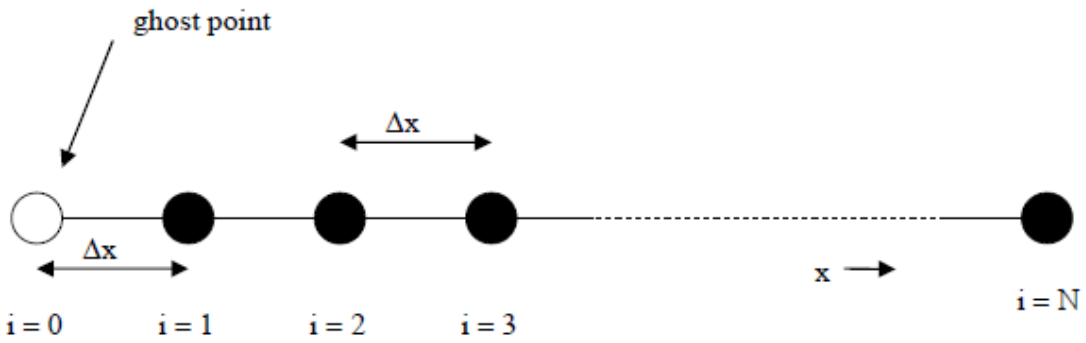

Figure 4.2: Ghost points [10]

at the grid points which are next to the ghost points ($i = 1$, corresponds to $x = 0$, $i = N$ corresponds to $x = 1$) [10]. So for the grid points $i = 1$ and $i = N$, the symmetric finite differences will be considered:

$$\left.\frac{\partial T(x,\tau)}{\partial x}\right|_{x=0} = T_x(x_0,\tau_n) = 0 \approx \frac{T_2^n - T_0^n}{2\Delta x} \tag{4.16}$$

$$\left.\frac{\partial T(x,\tau)}{\partial x}\right|_{x=1} = T_x(x_N,\tau_n) = 0 \approx \frac{T_{N+1}^n - T_{N-1}^n}{2\Delta x} \tag{4.17}$$

From these we obtain:

$$T_2^n = T_0^n, \quad T_{N+1}^n = T_{N-1}^n \tag{4.18}$$

By applying this approach to (3.41), (3.42), the following is obtained:

$$T_{2,2}^n = T_{2,0}^n, \quad T_{2,N+1}^n = T_{2,N-1}^n \quad T_{1,N+1}^n = T_{1,N-1}^n, \tag{4.19}$$

where the first lower subscript means the phase (1 is for fluid and 2 is for solid phase) and the second lower subscript is the number of spatial node. The superscript is the number of time node.

The first term in (3.42), i.e. $T_1(0,\tau) = 1$, is a *Dirichlet boundary condition*, and so the following difference is used [10]:

$$T_{1,0}^n = 1 \tag{4.20}$$

4.1.2 Stability analysis

For the stability analysis several methods can be used depending on the PDE and the used discretization method. Examples can be the well-known Von Neumann method, method using matrices or discrete perturbation method [19, 25]. In this thesis, only the Von Neumann method will be described shortly, other methods can be found in [19].

As it was mentioned at the end of section 4.1, instead of full discretization of equations (4.14), (4.15) only spatial discretization was done. These partially discretized equations were inserted into MATLAB using the solver ode45 which is designed to solve ordinary

differential equations. This solver also contains algorithms for solving stability and determining the size of the time step. Therefore, it is not necessary to explain the Von Neumann analysis in detail for this heat transfer problem, but it is enough to explain it in general.

4.1.3 Von Neumann analysis

This method of stability analysis is used when PDEs are being solved using some FDM. It belongs to the most common and most known methods of stability analysis. The principle of this method lies in the use of Fourier series and a so-called *amplification factor G*. The condition for the use of the Von Neumann stability analysis is linearity of the PDEs. For a non-linear PDE, the equation has to be locally linearized. The Von Neumann analysis can then be used piecewise on these locally linearized parts. It has to be noted that this obtained stability condition is valid only for the locally given part of the PDE.

After the use of a finite difference scheme on a PDE, the newly created finite difference equation will be expanded in a Fourier series and depending on the amplification factor, the FDM is either stable or unstable, depending on the growth or decay. The stability condition for the used FDM is generally given as $|G| < 1$. If the amplification factor has a real and imaginary part, the stability condition is given as $|G|^2 < 1$ [19].

5 Model setup

In this chapter the model of the packed bed will be modeled using all the information stated in the previous chapters. In the first step, tables with operation conditions, parameters of packed bed and thermophysical properties are listed. In the section 5.1, the numerical model is shown. In section 5.2, the results of the model are given.

The model created in this thesis is described by the data in Tables 5.1, 5.2 and by the equations (3.7)–(3.13). This model is based mainly on the information and model described in [21].

The model is based on forced convection where the hot air is pumped into to packed bed by a pump at a constant velocity, and so both convection and conduction are taken into account. It should be noted that only the charging cycle was considered.

As storage material were chosen granite pebbles. For simplicity were the pebbles considered as perfect spheres with a smooth surface. Pebbles are filled in the tube in a cubic arrangement. The data for granite were obtained from [22]. The pebbles have a diameter of 1.6 cm. As a heat transfer fluid was chosen dry air with properties obtained from [32].

From table 5.2 has the packed bed a length of 1 m with an inner diameter of 0.2 m. The inner wall thickness is considered negligible compared to the inner diameter. For this reason is the inner wall not considered in the computations. Thickness of the insulation is 0.25 m, so no heat loss (or a minimal one) is occurring. The total diameter of the vessel with insulation is 0.7 m.

The initial temperature of the packed bed and the pebbles was 27° C. After the pump was turned on, the dry air was flowing with a speed of 0.2 m/s and the air temperature was 127° C. The duration of the charging cycle was set for 2 hours.

Thermophysical properties of dry air and granite		
Dry air	**Value**	**Condition**
Inlet temperature $T_f(0,t)$	127 [° C]	none
Initial temperature $T_f(x,0)$	27 [° C]	none
Specific heat of $c_{p,f}$	1008 [J/kg·K]	none
Dynamic viscosity μ	$2.075 \cdot 10^{-5}$ [kg/m·s]	none
Thermal conductivity k_f	0.03 [W/m·K]	none
Density ρ_f	1 [kg/m^3]	none
Granite		
Initial temperature $T_s(x,0)$	27 [° C]	none
Specific heat c_s	859 [J/kg·K]	$25^\circ\,\mathrm{C} < T_s < 500^\circ\,\mathrm{C}$
Thermal conductivity k_s	3.125 [W/m·K]	$25^\circ\,\mathrm{C} < T_s < 500^\circ\,\mathrm{C}$
Density ρ_s	2550 [kg/m^3]	none

Table 5.1: Used thermophysical properties

Parameters of the packed bed		
Parameters of PB	**Value**	**Condition**
Length L	1 [m]	none
PB diameter d_t	0.2 [m]	none
Diameter of particles d_p	1.6 [cm]	$Bi < 0.1$
Voidage ε	0.4	$d_t/d_p \in [1.5, 50]$
Thermal conductivity of insulation k_{ins}	0.06 [W/m·K]	none
Heat transfer coefficient from insulation to ambient h_{ins}	4.49 [W/m^2·K]	none
Insulation thickness e	0.25 [m]	none
Parameters of particles		
Biot number Bi	0.141	$Bi < 0.1$
Effective thermal conductivity $k_{ef,s}$	0.81 [W/m·K]	$Re > 0.8$
Flow conditions		
Heat transfer coefficient for particles h_p	27.53 [W/m^2·K]	none
Heat transfer coefficient at wall h_w	22.02 [W/m^2·K]	none
Air velocity v	0.2 [m/s]	none
Pressure drop Δp	12.1 [Pa]	Δp is small
Reynolds number Re	61.6	none
Prandtl number Pr	0.6972	none
Nusselt number Nu	14.68	none
Effective thermal conductivity $k_{ef,f}$	0.64 [W/m·K]	$Re > 0.8$
Péclet number Pe	125	none
Particle stanton number Γ	77.02	none
Wall stanton number Γ_w	$9.28 \cdot 10^{-4}$	none
Overall heat transfer coefficient to ambient U_w	0.187 [W/m^2·K]	none

Table 5.2: Used parameters

In Table 5.1, for properties like air density, dynamic viscosity of dry air, thermal conductivity of dry air, no condition or restrictions of applicability were considered for the given values, since in section 2.4 it is considered that the air properties are constant (for model and computation simplification). If these properties should not be considered constant or some correlations would be used, then some temperature conditions for which these values are given should be stated (usually it would be a small temperature inter-

val since it was shown in section 2.4.1 that these properties are strongly temperature dependent).

For a heat storage problem such as this, it is also important to know the value of stored heat. Therefore, the formula from [18] was used:

$$\dot{Q} = \dot{m}\, c_f (T_i - T_o) \tag{5.1}$$

where $\dot{Q}$ is the *heat rate*, $\dot{m} = G \cdot A_0$ is the *mass flow rate*, T_i is the inlet fluid temperature and T_o is the outlet fluid temperature. To obtain the amount of stored heat, heat rate has to be integrated with respect to time, i.e.

$$Q = \int_0^t \dot{Q}\, dt = \int_0^t \dot{m}\, c_f (T_i - T_o) dt \tag{5.2}$$

5.1 Numerical model

The numerical model is based on the finite difference method described in section 4.1. So the temperature distribution in PB is calculated in spatial nodes x_i for $1 \leq i \leq N$. For the computation, 21 axial points were considered, each point 0.05 m far away from his neighboring points and therefore, $N = 21$. Also both left and right ghost point are considered, since a symmetric spatial difference was chosen. As it was said earlier, there is one exception for the left side (i.e. inlet of PB) for fluid temperature. This temperature is given by a BC which is $T_1(0, \tau) = 1$ at every time step. Since to plot temperatures at all times steps would be time-consuming, it was decided to plot only values at 600 time steps. This means that a time step of 12 s is used for plotting these values during the execution of the code.

The numerical model is described by the equations (4.14), (4.15) with boundary conditions (4.19), (4.20). As it was said in section 4.1.2, the stability analysis was not done since the equations (3.38) - (3.39) were discretized only in space. The stability condition was left for the solver ode45 in MATLAB to solve. The non-dimensional time $\tau = 0.44$ was used as the maximal time of heating cycle. In Figure 5.1, a piece of code used in MATLAB for solving this problem can be seen.

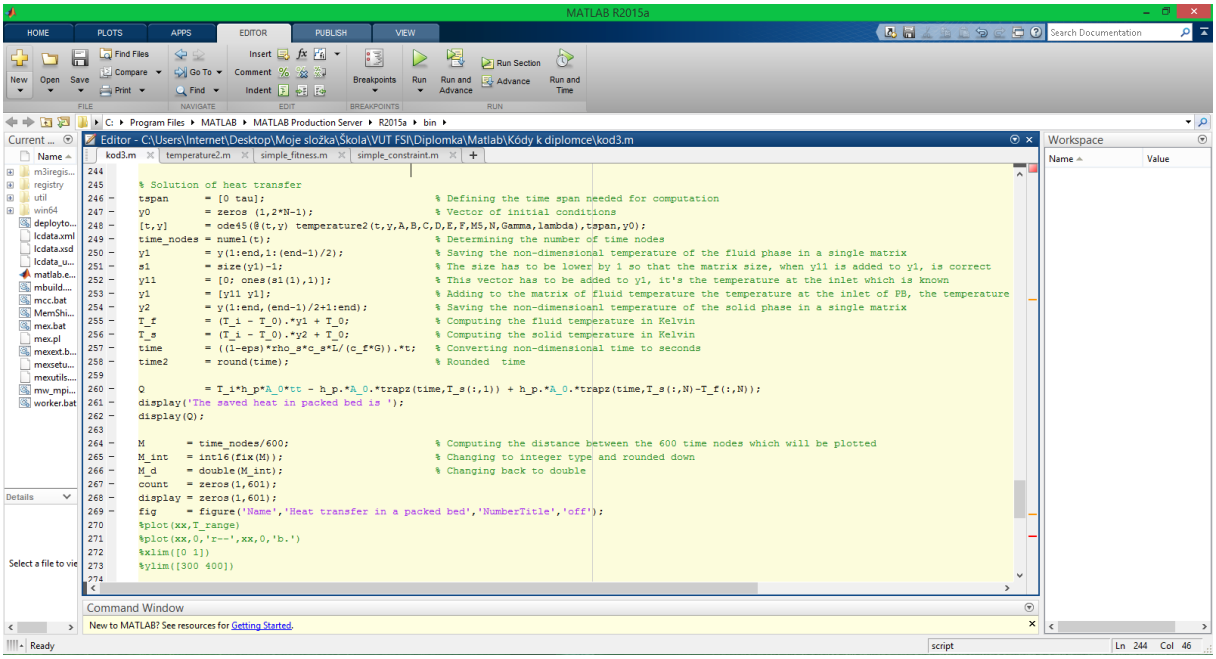

Figure 5.1: MATLAB code

To simplify the computations, the heat transfer was assumed to be one-dimensional, as well as the air flow. Also the air flow through PB is assumed to be fully developed and no transition zone is considered.

Since the PB contains pebbles, the flow has to be considered as a flow through porous medium and the usual heat conductivity of solid and fluid phase cannot be used, but instead an effective heat conductivity is needed. This is computed in section 3.4.1.

5.2 Result

As already said, MATLAB was used to compute this heat transfer problem. The computation of the whole code took 488 s. Below, six images can be seen with a temperature distribution at different time steps. All the images 5.2 – 5.8 are evaluated with the correlation of Nusselt number given in (3.20). These plotted images have a difference of 20 min since it would not be possible to fit all images into this thesis and representative samples were chosen.

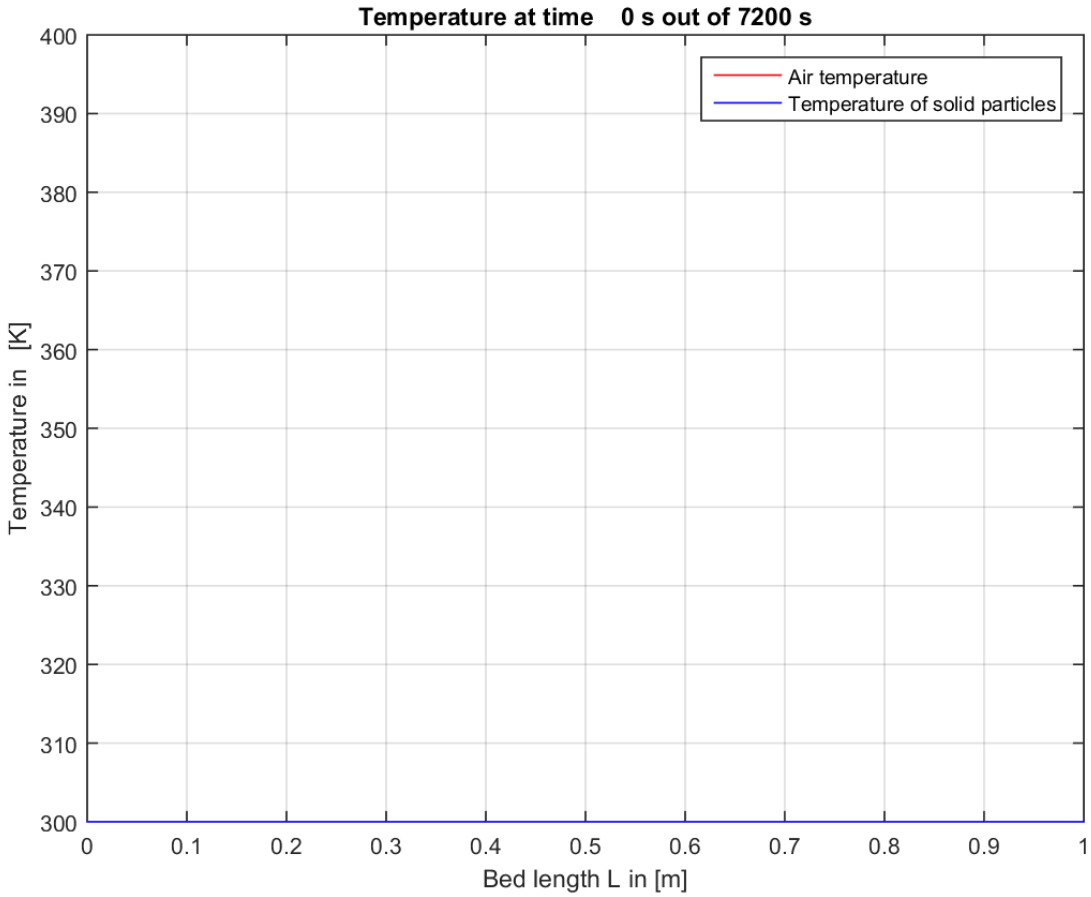

Figure 5.2: Temperature in the beginning

In the beginning, the IC (3.9) was that the temperature of both the fluid and solid phase is 0 which means it is at room temperature (for temperatures given in Kelvins, the value is 300 K). This can be seen in Figure 5.2. At the start of the heating cycle, the maximal temperature difference in whole PB between rock particles and hot air was 100 °C. In less than 3 minutes, this has dropped down to 50 °C. After 6 minutes of the beginning of the heating cycle, the temperature difference was around 20 °C. After approximately another 6 minutes, the difference is around 9 °C.

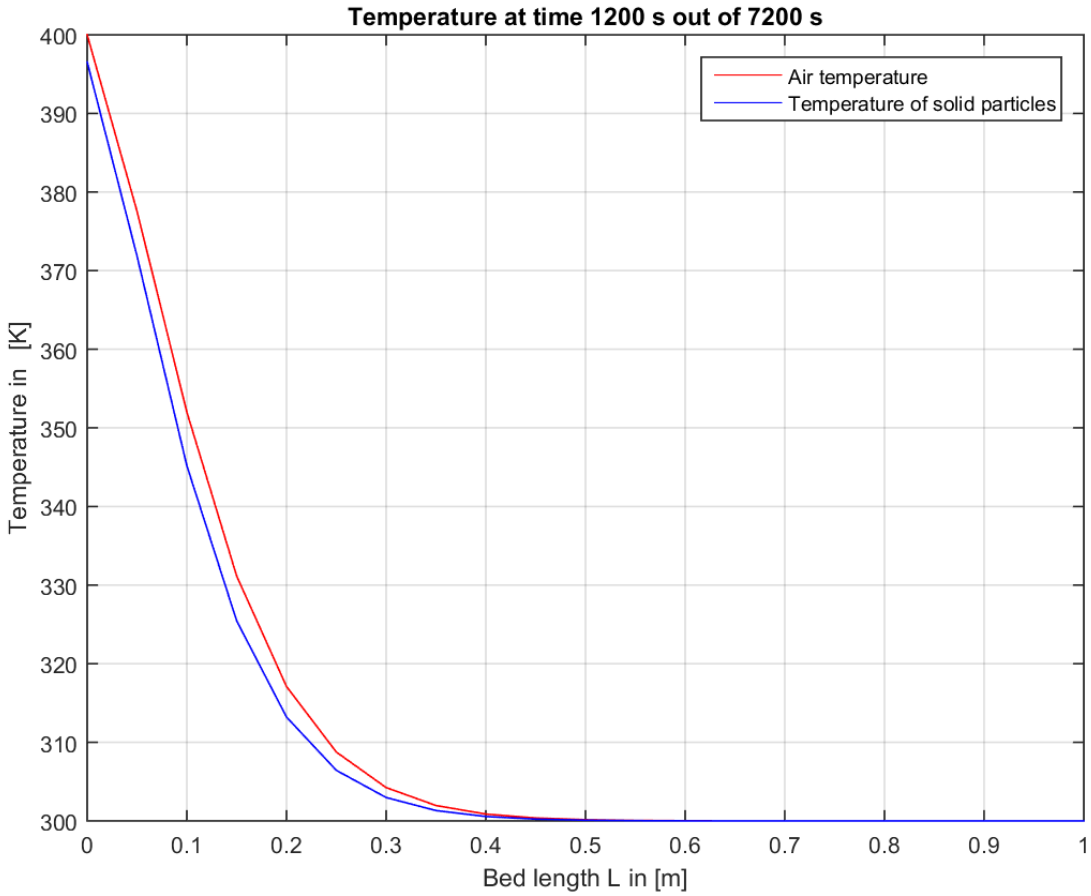

Figure 5.3: Temperature after 20 min of heating

In Figure 5.3, it can be seen that the fluid temperature at inlet is already 400°C. Temperature for both solid and fluid phase are decreasing exponentially. After heating the PB for about 20 minutes, only the first half of PB was heated, the second half of PB is still at its initial temperature. Also, the temperature difference is less than 7 °C.

In following Figures 5.4 – 5.8, it can be seen that the temperatures of both rock particles and air is rising, even though the rise is slow. This is due to the small air velocity. A small air velocity was chosen so that the pressure drop Δp is small and a big destruction of exergy does not occur. The value of the pressure drop is $\Delta p = 12.08$ Pa.

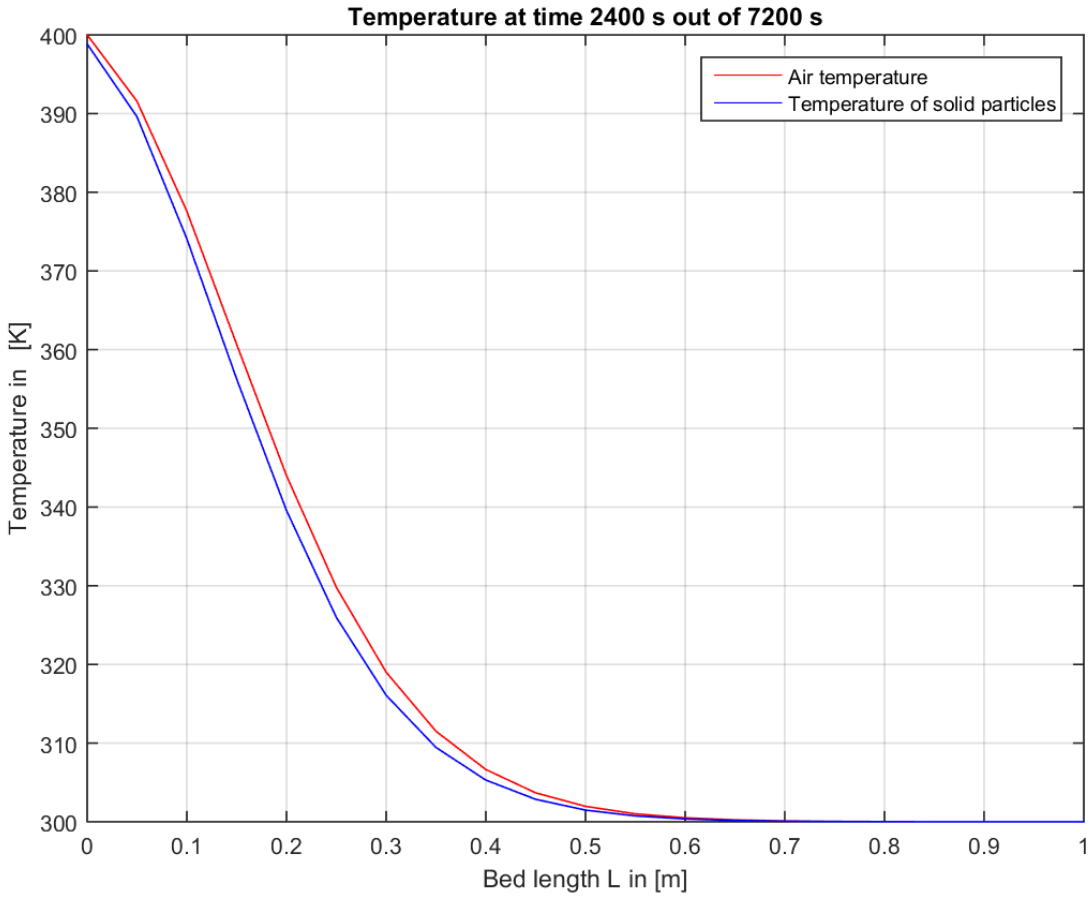

Figure 5.4: Temperature after 40 min of heating

In Figure 5.5, it can be seen that the temperature also started to rise in the middle of the PB, i.e. at $x = 0.5$ m. The temperature rise is only around 7 °C. Even after one hour of constant heating, most part of the second half of PB is at its initial temperature.

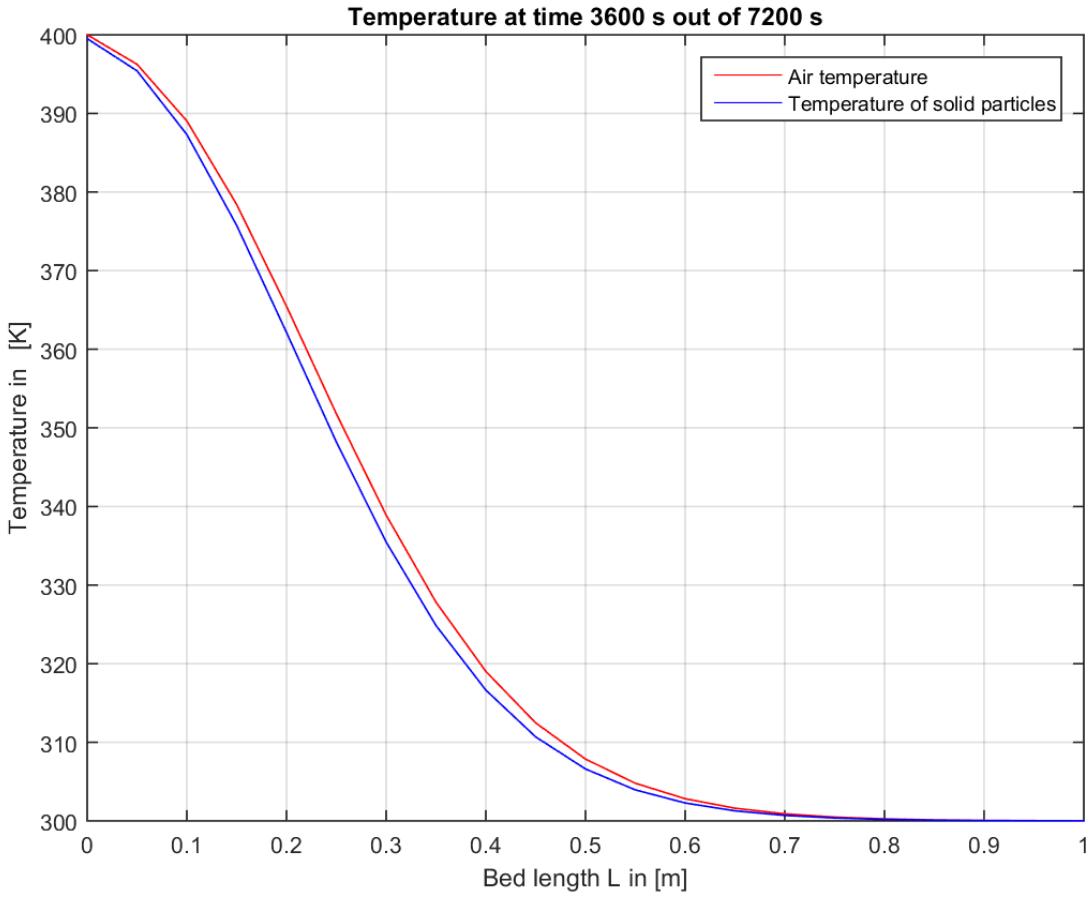

Figure 5.5: Temperature after 60 min of heating

In Figure 5.6, the temperature in the middle of the PB rose by approximately 17 °C. It can be also seen that the first 20 cm of the PB are heated to more than 100 °C.

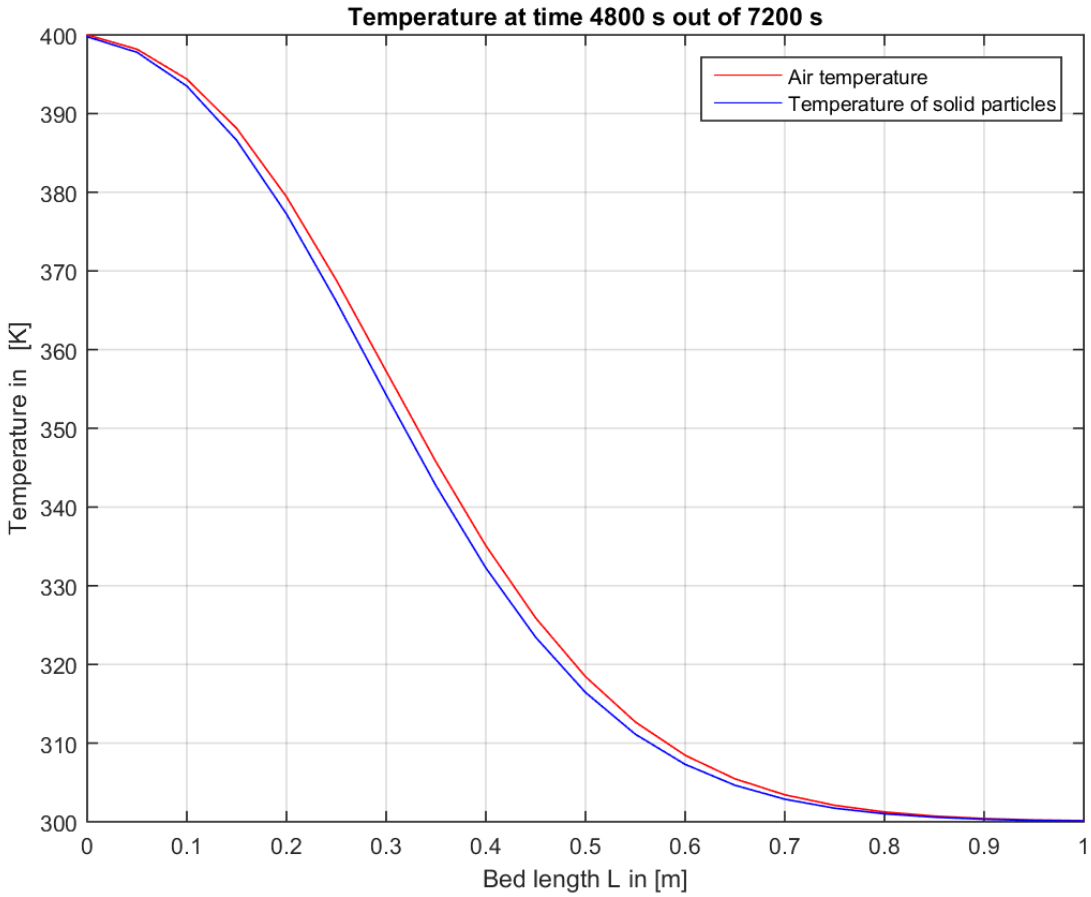

Figure 5.6: Temperature after 80 min of heating

In Figure 5.7, the temperature in the middle of the PB rose by approximately 30 °C.

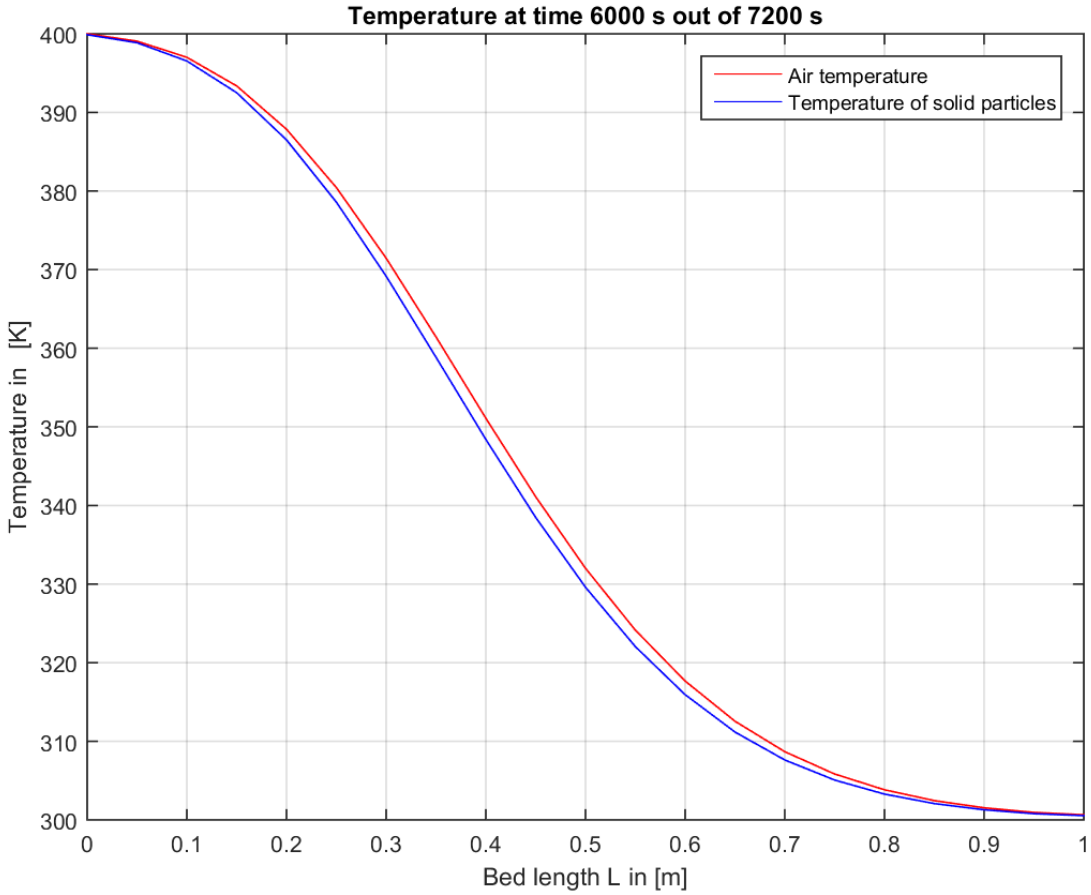

Figure 5.7: Temperature after 100 min of heating

In Figure 5.8, it can be seen that the temperature at the outlet of PB is around 305°C. To use the full potential of the PB, the heating cycle should be much longer than just 2 hours. The other way could also be to increase the air velocity but one has to be careful to not obtain a high value of pressure drop.

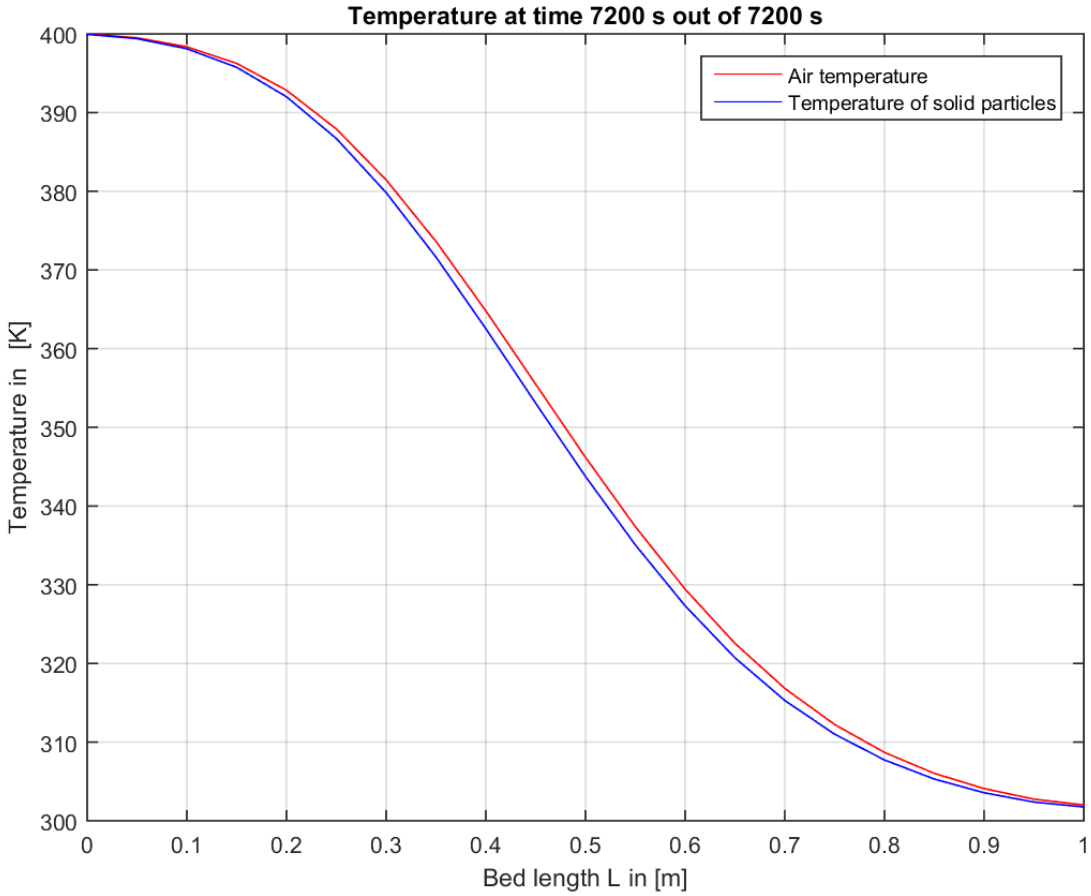

Figure 5.8: Temperature of both solid and fluid phase at the end

In images 5.2 – 5.8, it can be seen that the temperature of solid rock particles is close to the temperature of the air. The temperature difference has fallen to 5 °C after 30 minutes and was further dropping. After less than 75 minutes, the temperature difference was around 3 °C. This proves that an intra-particle thermal gradient is not necessary for the chosen parameters of PB and flow conditions since the temperature of the solid rock particles is changing fast enough in the whole interior. This was influenced by the small rock diameter which was $d_p = 1.6$ cm and also by small air velocity of $v = 0.2$ m/s. The total stored heat was computed with the formula (5.2): $Q = 1.816$ MJ.

The next task that was carried out was a comparison of 4 correlations for the Nusselt number *Nu*. These correlations are are given in (3.20) – (3.24). This is depicted in Figures 5.9, 5.10 and 5.11. As it can be seen, the plotted temperatures with different Nusselt numbers are very close. Therefore, only one correlation for Nusselt number can be used for the other computations. This chosen correlation is described in formula (3.20).

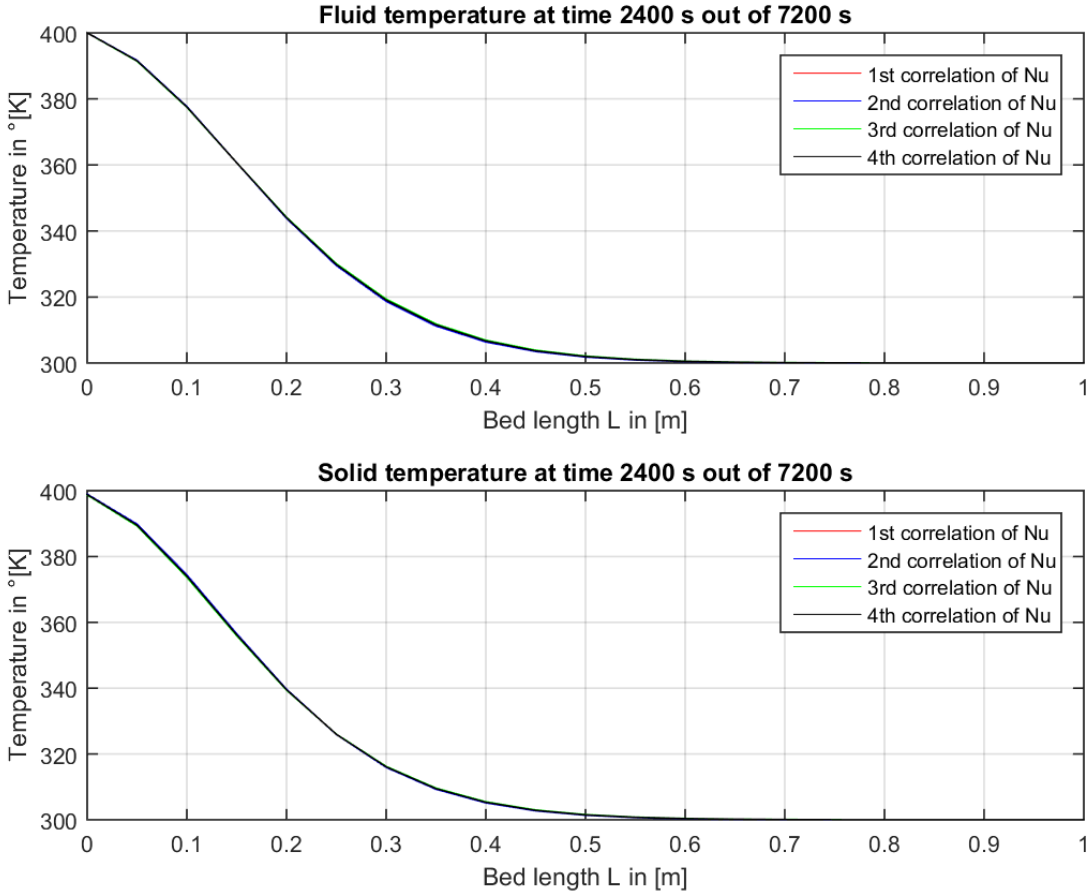

Figure 5.9: Temperature comparison with different Nusselt number

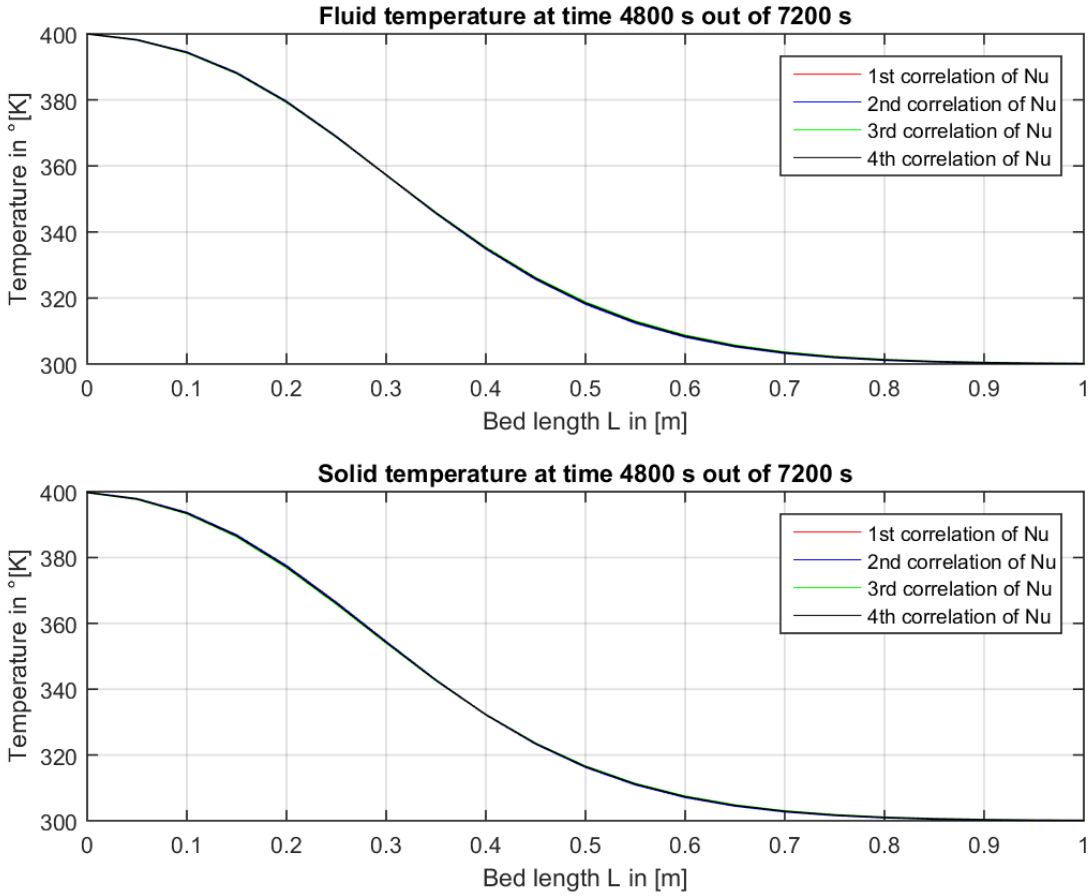

Figure 5.10: Temperature comparison with different Nusselt number

A comparison with real data would be useful, unfortunately no data with comparable parameters for PB and dimensionless numbers were found. Therefore, a validation with real data could not be done. The problem in finding suitable experimental data was that the found parameters and dimensionless numbers of other simulations were not similar. If the values would not be similar, the plotted temperatures would differ significantly.

It would be useful to remind what was explained in section 4, namely that all numerical simulations will always have at least slightly different results than exact solutions since numerical errors influence these simulations. Another reason can be all these simplifications done in order to obtain a faster and simpler algorithm.

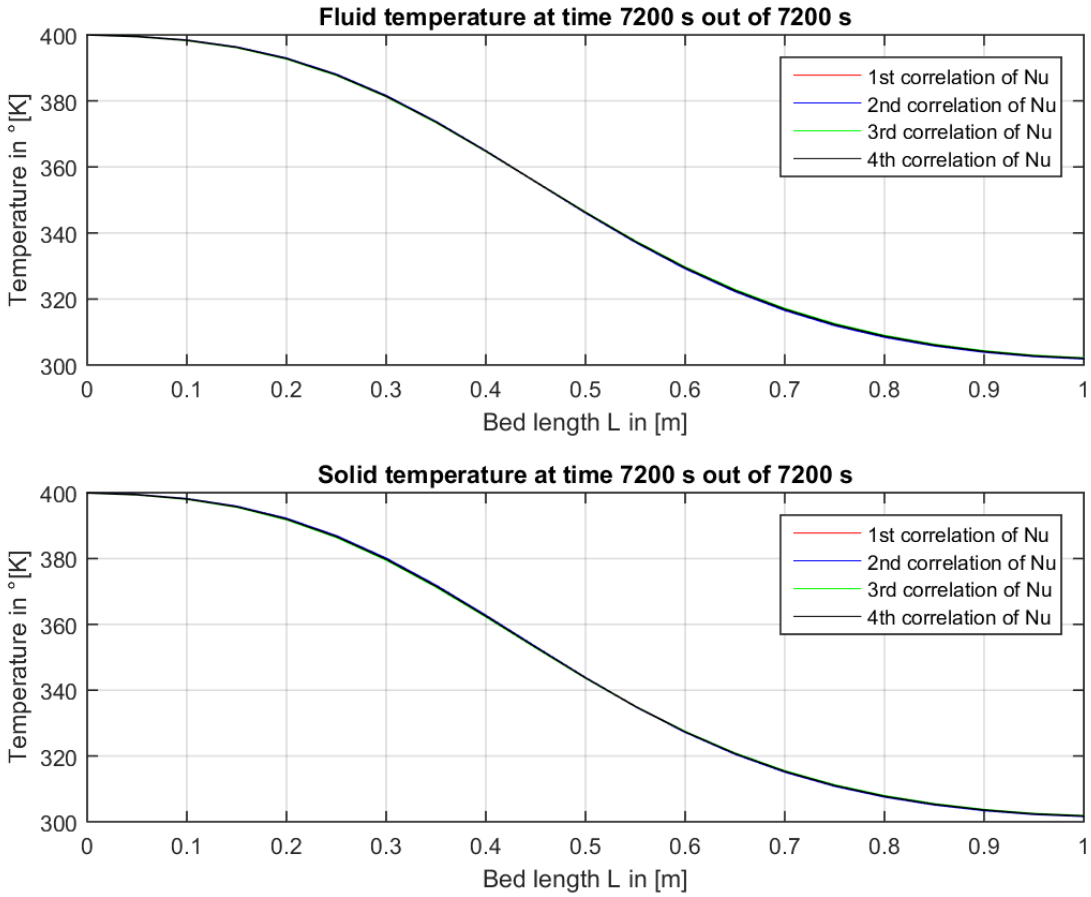

Figure 5.11: Temperature comparison with different Nusselt number

Another comparison can be time execution of the solver ode45 in MATLAB for different values of Nusselt number. The total execution time for all solvers is 124.1 s. For the first correlation with the value of $Nu = 14.68$ the execution time was 33.6 s, for the second correlation $Nu_2 = 15.68$ it was 32.2 s, for the third with value $Nu_3 = 13.66$ it was 28.9 s and the last Nusselt number, $Nu_4 = 14.51$, took approximately 29.4 s. So the execution times for different correlations of Nusselt number were influenced only little. This was expected since the Nusselt numbers vary only slightly. But since the Nusselt number depends on Reynolds and Prandtl number and these are computed from parameters like fluid velocity, particle diameter and thermo-physical fluid parameters, a bigger change in these parameter values could increase the execution time of the code.

The number of time nodes for all correlation of Nusselt number was around 200 000. This can be seen in Table 5.3, together with the execution times stated above.

Nusselt number	**Number of time nodes**	**Time**
Nu	209 161	33.6 s
Nu_2	218 309	32.2 s
Nu_3	199 837	28.9 s
Nu_4	207 629	29.4 s

Table 5.3: Evaluated time

From the total time of 488 s for the whole script, the most amount of time for this part of the algorithm took the plotting of temperatures which was 136.3 s.

6 Optimization

6.1 Introduction

By optimization, a procedure to obtain the best result for a given process is understood. Usually, the goal of optimization is to maximize the benefits or incomes, or to minimize the efforts spent for the process. So it can be understood as a procedure to find the maximal or minimal value of a function which describes the process.

There are two major groups of optimization methods: exact method which are giving the best exact solution for a given problem and approximate methods which are not giving an exact optimal solution but an approximate one [27].

In Figure 6.1 are shown the various categories of optimization methods. For this thesis, the genetic algorithm from the group of population-based metaheuristics has been used.

As the first step, the problem has to be formulated. Second, a mathematical model which describes the problem is made. Usually to solve the problem in a reasonable time, it has to be simplified. As the next step, the simplified problem is optimized. Depending on the used algorithm, an exact or satisfactory result is obtained. It has to be taken into account that the model was simplified, and so the optimal solution is not related to the original problem. The optimal solution just indicates when is the model accurate. Lastly, the solution has to be tested, and if it is acceptable, it will be implemented into the original model. If it is not acceptable, the model or the used algorithm (or both) have to be changed and the whole process has to be repeated [12].

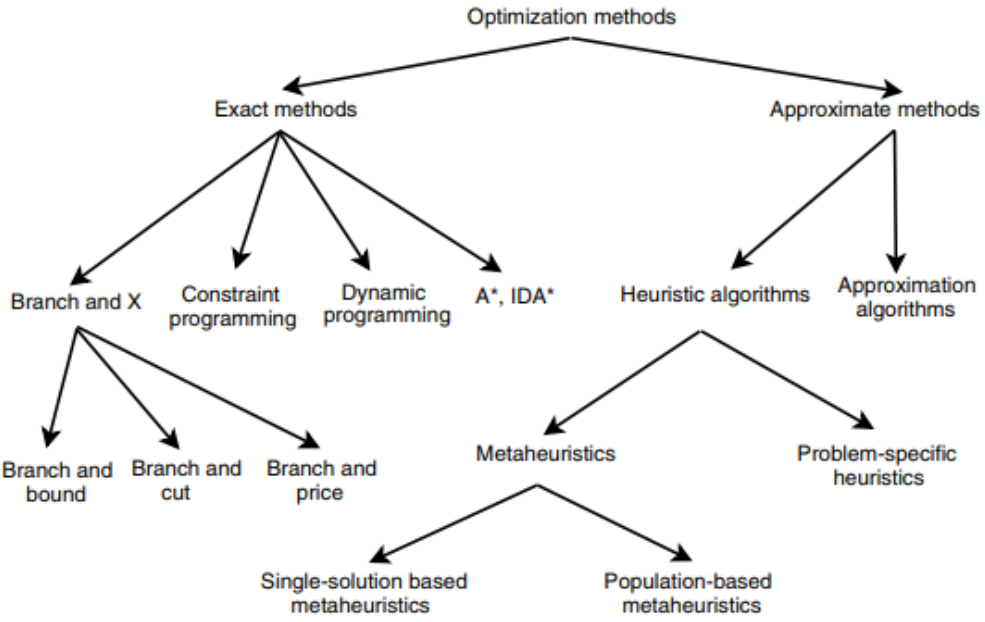

Figure 6.1: Optimization algorithms [12]

6.2 Metaheuristics

Metaheuristics are approximate optimization algorithms (do not confuse with approximation algorithms) which are not giving the best possible optimal solution, but are providing a satisfactory solution in a reasonable time for large scale problems. But for metaheuristics, there is no guarantee to find global optimal solutions or bounded solutions. Compared to approximation algorithms, metaheuristics do not provide a measure of how close the obtained solutions are with respect to the optimal solutions [12].

Further, it is also important to give a basic description of a *black box function* which will be later used to optimize the heat transfer problem:

Definition 3. A function $f : X \to R$ is called a *black box function* if and only if the following conditions are satisfied:

- the domain X is known
- it is possible to know the function f for each point of X
- no other information is known about f

So from this definition we get that an objective function is an black box if the objective function cannot be expressed analytically. So for a black box function we know the input and output [12].

6.3 Population-based metaheuristics

To talk about population-based metaheuristics, the notion of the *search memory* will be needed:

Definition 4. The *search memory* (or just simply *memory*) is a set of information which is obtained and saved during the search, for example in evolutionary algorithms the memory is a population of individuals [12].

These algorithms are using a population of solutions and the optimal solution is obtained by an iterative improvement of such a population. As a first step, an initial population is generated. As the second step, before the new population is generated, some solutions (in this case the parents) from the current population have to be chosen by using some selection strategy and this parents are allowed to reproduce themselves, i.e. to generate new offsprings. This is done by using some reproduction algorithm, for evolutionary algorithms it is in general a binary operator. Third, a new population is generated. The newly generated population is then implemented into the first one and a new solution has to be selected from the current population and the generated one using some replacement strategy. Usually, the generated population is chosen but also the better solution of the two can be taken. As the last step, the search memory is updated with the new population. To stop this algorithm, a stopping criterion has to be satisfied. There are several stopping criteria: exceeding a given number of population which are generated,

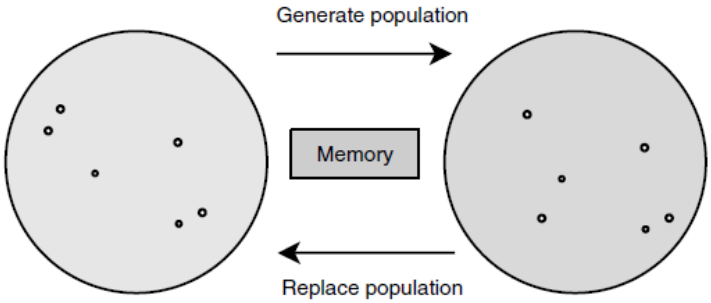

Figure 6.2: Population-based metaheuristics [12]

maximum number of objective function evaluations,etc. Another kind of stopping criteria could be linked to population diversity, e.g. when the population is stagnating.

The generation (reproduction) and implementation (or also replacement) phase can be either memoryless, meaning that both phases are dependent only on the current population, or memory dependent. In this case some history can be used in the generation and replacement phase [12].

The most known algorithms from this category are evolutionary algorithms, scatter search, particle swarm optimization, bee colony, etc.

The generation of the *initial population* is important for the algorithm to be effective. The crucial criterion is that the initial population is well diversified. If this criterion will not be satisfied then a premature convergence can occur. There are 4 groups of initial population generation: random generation, sequential diversification, parallel diversification and heuristic initialization [12].

As the name indicates, *random generation* is generating the initial population randomly. The most used algorithm for random generation is using pseudo-random numbers. Another option is to use a quasi-random sequence of numbers. This option has a better diversity compared to the pseudo-random numbers. *Sequential diversification* generates a sequence of solutions where the diversity is optimized. The *parallel diversification* is using parallel generated population and the last group is *heuristic initialization* which is using heuristics to generate the initial population. The disadvantage of last named group is that the initial population may lose diversity [12].

6.3.1 Genetic algorithms

Genetic algorithms are one of the most popular and most used algorithms from the group of evolutionary algorithms. It is using a crossover operator (for the two main solutions) and a mutation operator for the reproduction phase. The mutation is randomly changing an individual so that the diversity is satisfied [12].

First, some basic notion will be introduced:

Definition 5. An *individual* is every solution to the optimization problem. The set of all individuals is called a *population* [18].

Definition 6. A *fitness function* is any function which is measuring suitability of an individual for a given optimization problem and its value is called *fitness* [18].

The genetic algorithms are starting with an empty population of offspring. As the next step, two parents are selected from the initial population and by using crossover we reproduce the parents and use the mutation operator to change the offspring. As a result, two individuals are generated in the new population. This procedure is repeated until the new population is full [24].

This algorithm is described in Figure 6.3:

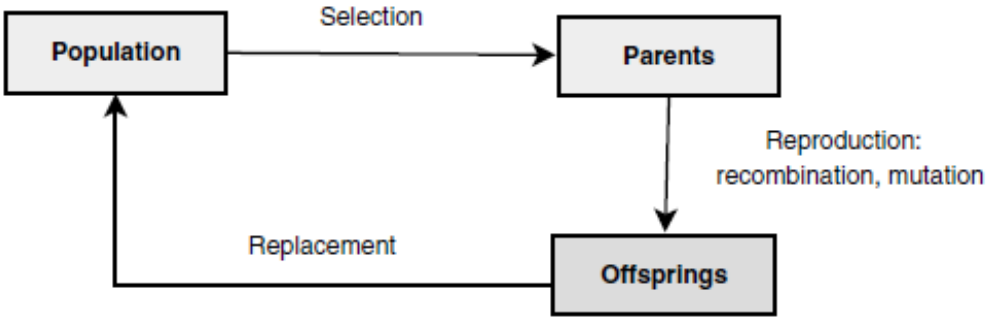

Figure 6.3: Principle of Genetic Algorithms [12]

Selection phase

For the genetic algorithms, there are several selection strategies: *Roulette Selection*, *Stochastic Universal Sampling*, *Tournament Selection*.

The Roulette Selection (known also as Fitness-Proportionate Selection) is selecting the individuals depending on their fitness. The higher the fitness value, the more often is the individual selected. For this, we determine the size of each individual depending on their fitness value. The sum of all fitnesses is denoted as s. If a random number $r \in [0, s]$ falls into the area of an individual, then this individual is selected [24]. In other words, the probability that an individual is selected is given by the probability

$$p_i = \frac{f_i}{\sum_{j=1}^{n} f_j},$$

where i is the given individual, f_i is its fitness and n is the number of individual in the current population P. For selecting k individuals ($k \leq n$) from the current population, the procedure has to be repeated k times [12].

Similar to this is the Stochastic Universal Sampling algorithm, but all individuals which are fit are selected at least once. The algorithm works as follows: Just like for the Roulette Selection, the individuals are determined by their size, based on the individual fitness. If a random number $r_1 \in [0, s/n]$, where n is the size of the next generation, falls into the area of an individual, then this individual is selected and the number r_1 is added to s/n. We then choose $r_2 \in [0, q]$, where $q = s/n + r_1$. This procedure is repeated n times [24].

The Tournament Selection is choosing an individual with the best fitness from a group of t individuals which are chosen randomly. The number $t \geq 1$ is the tournament size. For selecting k individuals ($k \leq n$) from the current population, the procedure has to be repeated k times. This algorithm is the most used one, since it has 3 advantages compared

to the previous algorithms: it is not sensitive on the fitness function, it is simpler than the first two algorithms and we can choose an arbitrary tournament size [12, 24].

Reproduction (or generation) phase

The crossover operation is made by mixing and matching of two parents and it depends on the individuals. For using crossover on vectors either *one-point*, *two-point* or *uniform* crossover can be used. For the one-point crossover, two parent which are described by vectors x and y, respectively, have to consider where both vectors are of the length l. The algorithm is starting with choosing a position $c \in [0, l]$. For every position which is smaller than c, the value of the given position between vector x and vector y are swapped. If $c = 1$ then no swapping occurs. This happens with a probability of $\frac{1}{l}$. Similar to the one-point crossover is the two-point crossover but instead of choosing only one position c, two positions are chosen: c and d. The values of x and y with positions which lie between c and d are then swapped. This way, a multi-point crossover with n positions: $c_1, c_2, ..., c_n$ can be introduced. The positions in x and y which are between c_1 and c_2, c_3 and c_4,..., c_{n-1} and c_n will be swapped. The uniform crossover is not using the segment size of the individuals and so for the generation of an offspring, each parent contributes to the offspring equally [24].

An alternative to crossover operation could be an algorithm called as *Line Recombination* where the vectors of both parents are represented as two points in space and a line is drawn between those two points (the line can be extended beyond the points as well). The offspring is lying on the lines and depending on the value p, the offspring can lie between the two points (for p = 0) or it can lie anywhere on the line, even beyond the points (when $p > 0$) [24].

The mutation operator is an unary operator, i.e. it is operating with only one individual. It is recommended that the mutation operator has a small probability to change an individual, in general it could be $p_i \in [0.001, 0.01]$, where i is the given individual [12, 24]. For a vector of real values, the mutation can be done by Gaussian convolution, and for a boolean vector a bit-flip mutation can be used. Both algorithms are described in [24].

Replacement phase

The goal of this phase is to select the individuals for the new population (can be also understood as the survival of the fittest individuals). These are selected between the individuals of the current population and their offsprings. We differ between deterministic or stochastic replacement strategies. For a constant population, the offsprings are replacing their parents one by one. There are two main strategies: *Generational replacement* and *Steady-state replacement*. For the first mentioned strategy, the parent population is completely replaced by the offspring population, meaning that all parents are replaced by their offsprings (the number of offsprings is the same as the number of parents). Using the steady-state replacement, the new population consists of all parents, except for the worst individual from the parent population which is replaced by an offspring. This means that only one offspring is generated.

There are further strategies which are lying between those two mentioned earlier. In other words, these strategies are replacing b individuals from the current population of a individuals ($1 < b < a$), (with different b, different strategies are obtained).

The elitism replacement is selecting only the fittest individuals among both parents and their offsprings. These individual with the best fitness are called *elites*. The problem of elitism is, if it is not controlled, it could lead to a premature convergence. In other words, to restrict premature convergence, individuals with a bad fitness have to be chosen, too. Another way would be to increase the reproduction noise [12, 24].

6.4 Model optimization

Another goal of this thesis was to optimize the established model which will be done in this section. For this goal, the solver ga in MATLAB was utilized. This solver is part of the Optimization Toolbox in MATLAB.

The optimization used in this thesis is based on the Genetic algorithm from the family of population-based Metaheuristics described in section 6.3.

To optimize the given problem, two possible ways are available. The first option is to maximize the stored heat Q for a given time which would be $t = 7200$ s. The only parameters that would be optimized are particle diameter d_p, air velocity v and inlet fluid temperature T_i. The second option is to minimize time t needed for the heating cycle to obtain a certain level of stored heat Q. The optimized parameters are the same as in the first option, i.e. d_p, v and T_i. These parameters have to be limited with some conditions. Otherwise, these optimized parameters could be optimized unrealistically, for example the particle diameter would be bigger than the diameter of PB or the inlet fluid temperature would have thousands of degrees Celcius, etc. For this thesis, the first option was chosen, i.e. maximization of stored heat Q.

For design optimization, also other parameters than d_p, v and T_i could be used, namely the length of packed bed L or diameter of packed bed d_t.

As it was said in [27], maximizing an objective function $f(x)$ is the same as minimizing $-f(x)$. This optimization problem can be written as

$$\max_{\mathbf{x}} \quad \mathrm{Q} = \min_{\mathbf{x}} \quad -\mathrm{Q} \tag{6.1}$$

where $\mathbf{x}$ is the vector of parameters to be optimized.

With the use of formula (5.2), it gets the shape as

$$\begin{aligned} \min_{\mathbf{x}} \quad -\mathrm{Q} &= -\int_0^t \dot{m}\, c_f (T_i - T_o) dt \\ &= -\int_0^t G A_0\, c_f (T_i - T_o) dt \end{aligned} \tag{6.2}$$

To obtain a dependency of heat on particle diameter, the formulas (2.9) and (3.2) have to be used. This will result in

$$\begin{aligned} -\int_0^t GA_0\, c_f(T_i - T_o)dt &= -\int_0^t \rho_f\, v\, \varepsilon\, A_0\, c_f\, (T_i - T_o)dt = \\ &= -\int_0^t \rho_f\, v \left(0.39 + \frac{1.74}{\frac{d_t}{d_p} + 1.14}\right)^2 A_0\, c_f\, (T_i - T_o)dt \end{aligned} \tag{6.3}$$

This way the optimization problem 6.1 can be rewritten in the form

$$\min_{\mathbf{x}} \quad -\int_0^t \rho_f\, v \left(0.39 + \frac{1.74}{\frac{d_t}{d_p} + 1.14}\right)^2 A_0\, c_f\, (T_i - T_o)dt \tag{6.4}$$

To use an optimization algorithm in MATLAB, it is necessary to rewrite the optimized parameters T_i, v and d_p as unknown parameters of vector $\mathbf{x}$= ($x(1)$, $x(2)$, $x(3)$), where $x(1) = T_i$, $x(2) = v$, $x(3) = d_p$. The boundary of these parameters were set in the following way:

$$300 \text{ K} \leq T_i \leq 450 \text{ K}$$
$$0 \text{ m/s} \leq v \leq 0.3 \text{ m/s}$$
$$0 \text{ m} \leq d_p \leq 0.02 \text{ m}$$

The final form of the optimization problem is

$$\min_{\mathbf{x}} \quad -\int_0^t \rho_f\, x(2) \left(0.39 + \frac{1.74}{\frac{d_t}{x(3)} + 1.14}\right)^2 A_0\, c_f\, (x(1) - T_o)dt \tag{6.5}$$

The first boundary condition is for the inlet fluid temperature. The lower boundary is set to 300 K which is approximately 27°C and is the initial HSU temperature. If it would be lower than 27°C, it would mean that cooling of the packed bed is allowed, which is undesirable. The upper boundary is set to 450 K, approximately 150°C. This was chosen with respect to the fact shown in section 2.4, namely that the thermo-physical properties of air change with increasing temperature. For simplicity though, a constant value for used thermo-physical properties was assumed. If a higher upper bound should be used, variable temperature-dependent thermophysical properties would have to be used so that the accuracy is not decreased.

Second boundary condition is used for air velocity. From a physical point of view, it would not be possible to have a negative air velocity. That is the reason for the lower boundary condition to be non-negative. The upper boundary is again chosen with respect to pressure drop, since a higher velocity also means higher pressure drop. Therefore, only a slightly higher velocity of 0.3 m/s was considered.

Third boundary condition is for particle diameter. This condition is also essential since particles with big diameter would not satisfy the condition for Biot number. Again, lower boundary is set to be non-negative, since spheres cannot have negative diameters. Upper boundary is, as it was said, considered to satisfy the Biot number. The value is 2 cm.

6.5 Result

With the use of the solver ga and the Optimization Toolbox in MATLAB, the result for the optimization part will be discused in this section.

Script-based optimization

The first optimization cycle/trial was done as a script in MATLAB. The settings for Selection and Reproduction phase were left default. The results from the script are following:

Number of generations	5
Number of function evaluations	13 050
Execution time	95.8 s

Table 6.1: Performance in script

The amount of stored heat was 2.507 MJ. Compared to the result without optimization, the increase is around 38 %. The optimised parameters have following values:

- $T_i = 423.15$ K
- $d_p = 0.02$ m
- $v = 0.3$ m/s

The reason why the cycle stopped was because the average change in the fitness value was less than the default tolerance of the solver.

These values were expected since, as it was shown in section 5.2, the potential of the PB was not completely used, i.e. with a higher air velocity, more hot air would be pumped into PB and therefore, also more heat would be stored in the second half of PB. In Figures 5.2 – 5.8, it can be seen that in the second part of PB, the temperature is still low, even after a heating cycle of 2 hours.

As for the optimized air inlet temperature, this result was also something that could be intuitively predicted since a bigger temperature means also more stored heat.

Toolbox-based optimization

As it was said above, for the next cycles, the Optimization Toolbox was utilized. First, three cycle were running with default settings where a Stochastic uniform selection was chosen. This selection is described in the subsection **Selection phase** of the section 6.3.1.

The results of performance can be seen in Table 6.2.

Parameter	First trial	Second trial	Third trial
Number of generations	117	135	170
Number of function evaluations	5900	6800	8550

Table 6.2: Performance in Toolbox

For these cycle in the Optimization Toolbox, the results were the same as the results obtained in the script, i.e. T_i, d_p, v and Q have the same value. The performance of the second trial is depicted in Figure 6.4.

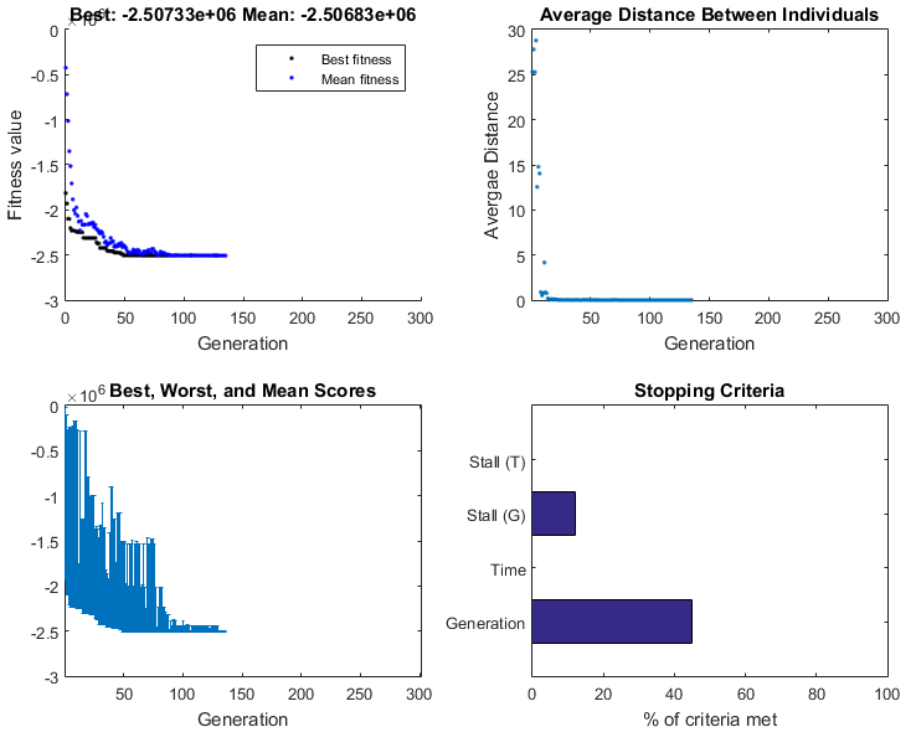

Figure 6.4: Cycle using the Optimization Toolbox

Another cycles in Optimization Toolbox were done but this time the Tournament selection with tournament size 1 was chosen.

The performance results of these cycles are described in Table 6.3. It should be noted that the optimized values of d_p and v were the same as for the script. The first trial of these cycles is shown in Figure 6.5.

Parameter	First trial	Second trial	Third trial
Number of generations	210	174	181
Number of function evaluations	10 550	8750	9100
Optimized inlet air temperature	411 K	421.8 K	419.6 K
Optimized stored heat	2.26 MJ	2.48 MJ	2.43 MJ

Table 6.3: Performance in Toolbox using Tournament selection

The reason why all the cycles stopped was because the average change in the fitness value was less than the default tolerance of the solver.

These results vary from the results obtained in the cycles where the Stochastic uniform selection was chosen in the value of optimized parameters, namely the inlet air temperature T_i which is 411 K for the first trial, 421.8 K for the second and 419.6 K for the third one. Therefore, also the stored heat Q is different from the results obtained in the script. This can be explained by the nature of the Tournament selection which was also described in section 6.3.1. Basically, the cycles using Tournament selection with a tournament size $t = 1$ select each generation one individual with the best fit from a group of t individuals. This means that a tournament of size 1 is too narrow, i.e. that there are not enough individuals from which the algorithm could choose the best fit. So it is appropriate to choose a bigger tournament size.

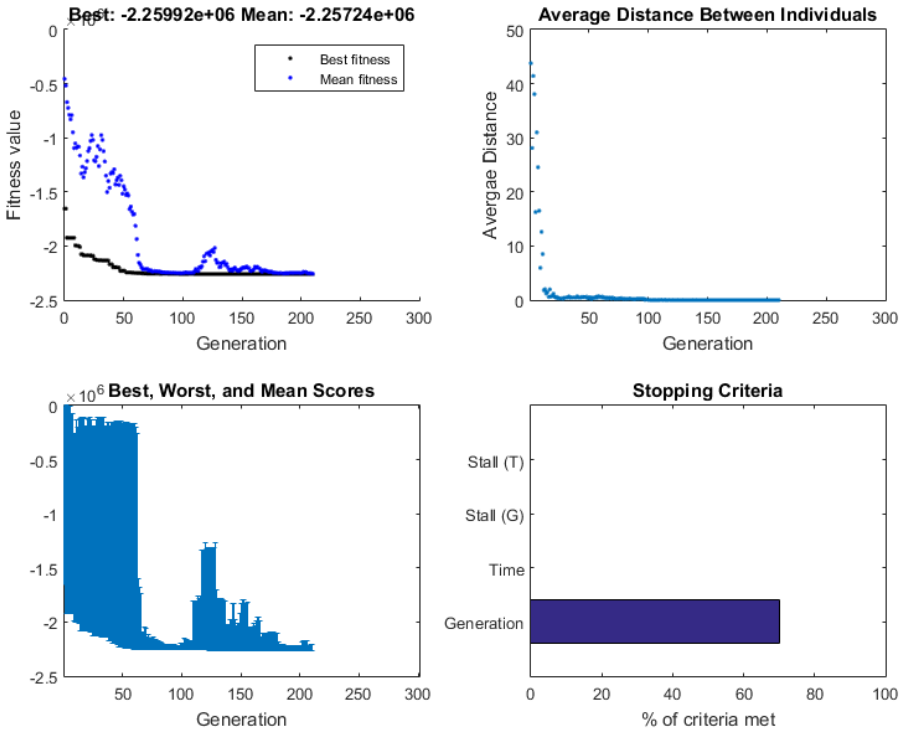

Figure 6.5: Cycle using tournament as selection

It should also be noted that even though the settings for the optimization are the same, every cycle has a different performance and different results since every optimization cycle using the Genetic Algorithm is unique, i.e. every new cycle is generating a bit different individuals and therefore, also the execution times are different. These individuals influence the whole optimization process. So the conclusion for these results are that using the Stochastic uniform selection, all the trials obtained the same results for the optimized parameters. The only values that were different, were number of generations and number of function evaluations. As for the Tournament selection, different values for heat and air inlet temperature were obtained. This is due to a small tournament size ($t = 1$).

7 Conclusion

The first goal of this Master's thesis was to set up a numerical model of a heat storage unit of the type packed bed and to create a computer simulation which is showing the temperature distribution inside of the packed bed. The second goal was to do a design optimization for this numerical model. Both task were carried out in a program chosen by student's preferences which was MATLAB.

The first task was done in section 5.1 and the result were presented in section 5.2. Model of this HSU was developed using a one-dimensional continuous solid phase model. For the numerical simulation, the finite-difference method was used. The temperatures of the fluid and solid phase were close and therefore the use of the term for intra-particle gradient was not necessary. Also, the pressure drop attained a low value and the use of counter-measures to decrease the pressure drop was not necessary. After 2 hours of heating, the PB was not fully heated due to low air velocity and a short time of the heating cycle. Unfortunately, no real data were found for comparison and therefore, the confirmation of the obtained results could not be done.

As for the second part, the design optimization was conducted in section 6.4 where also the procedure was described. The results from the optimization were shown in section 6.5. For optimization, a code was developed as a part of the thesis. Also the Optimization Toolbox from MATLAB was utilized. Several trials were conducted in order to gain an overview in precision and performance by using the Genetic algorithm. Two Selection processes were utilized, namely the Stochastic uniform selection and Tournament selection. Using the first named selection, all trials achieved the same optimized values, except for the performance which depends on the generated individuals. The Tournament selection with tournament size of one individual obtained slightly different values for air inlet temperature and therefore also the amount of stored heat was different. Nevertheless, the obtained results are in agreement with other results.

This thesis presented the topic of heat storage and could be used for other practical issues concerning heat storage via sensible heat. It also offered a better understanding of topics like heat storage, numerical methods and mathematical modelling of real-life problems.

A few recommendations for future works could be the creation of an user interface where the user would have a table and would be able to insert his preferred dimensions, flow conditions, etc. Also other shapes of solid particles could be used, e.g. bricks, ellipsoids, cubes, etc. This would need the use of a parameter called *sphericity*. Concerning the solid particles, also particles of non-homogeneous size, so-called *bi-sized particles* could be considered. For the code itself, it would be also good to consider an optimization of the execution time of the code. Considering the mathematical models, one could also compare precision and performance of models like Schumann's model, two-dimensional continuous solid phase model with the current one.

8 Bibliography

[1] J. Almendros-Ibáñez, M. Fernández-Torrijos, M. Díaz-Heras, J. Belmonte, and C. Sobrino. A review of solar thermal energy storage in beds of particles: Packed and fluidized beds. *Solar Energy*, vol. 192:pp. 193–237, 2019. DOI = 10.1016/j.solener.2018.05.047, Available at: `https://doi.org/10.1016/j.solener.2018.05.047`.

[2] R. Anderson, L. Bates, E. Johnson, and J. F. Morris. Packed bed thermal energy storage: A simplified experimentally validated model. *Journal of Energy Storage*, vol. 4:pp. 14–23, 2015. DOI = 10.1016/j.est.2015.08.007, Available at: `http://dx.doi.org/10.1016/j.est.2015.08.007`.

[3] R. Anderson, S. Shiri, H. Bindra, and J. F. Morris. Experimental results and modeling of energy storage and recovery in a packed bed of alumina particles. *Applied Energy*, vol. 119:pp. 521–529, 2014. DOI = 10.1016/j.apenergy.2014.01.030, Available at: `http://dx.doi.org/10.1016/j.apenergy.2014.01.030`.

[4] J. Beek. Design of Packed Catalytic Reactors. *Advances in Chemical Engineering*, vol. 3:pp. 203–271, 1962. DOI = 10.1016/S0065-2377(08)60060-5, Available at: `https://doi.org/10.1016/S0065-2377(08)60060-5`.

[5] F. Benyahia and K. E. O'Neill. Enhanced voidage correlations for packed beds of various particle shapes and sizes. *Particulate Science and Technology*, vol. 23:pp. 169–177, 2005. DOI = 10.1080/02726350590922242.

[6] T. L. Bergman and F. P. Incropera. *Fundamentals of heat and mass transfer*. John Wiley & Sons, Hoboken, New Jersey, 7th edition, 2011. 1048 p., ISBN = 978-0470-50197-9.

[7] H. Bindra, P. Bueno, J. F. Morris, and R. Shinnar. Thermal analysis and exergy evaluation of packed bed thermal storage systems. *Applied Thermal Engineering*, vol. 52(2):pp. 255–263, 2013. DOI = 10.1016/j.applthermaleng.2012.12.007, Available at: `http://dx.doi.org/10.1016/j.applthermaleng.2012.12.007`.

[8] R. P. Canale and S. C. Chapra. *Numerical methods for engineers*. McGraw-Hill, New York, 6th edition, 2010. 968 p., DOI = 10.1016/0378-4754(91)90127-o.

[9] M. Ö. Çarpinlioğlu, E. Özahi, and M. Y. Gündoğdu. Determination of laminar and turbulent flow ranges through vertical packed beds in terms of particle friction factors. *Advanced Powder Technology*, 20(6):515–520, 2009. DOI = 10.1016/j.apt.2009.06.006, ISSN = 09218831, Available at: `https://doi.org/10.1016/j.apt.2009.06.006`.

[10] D. M. Causon and C. G. Mingham. *Introductory finite difference methods for PDEs*. Ventus Publishing ApS, 2010. 125 p., ISBN = 978-87-7681-642-1, Available at: `https://bookboon.com/en/introductory-finite-difference-methods-for-pdes-ebook`.

[11] Y. A. Çengel. *Heat Transfer: A Practical Approach*. McGraw-Hill, Boston, 2nd edition, 2003. 896 p., ISBN = 9780072458930.

[12] El-Ghazali Talbi. *Metaheuristics from design to implementation*. John Wiley & Sons, Inc., Hoboken, New Jersey, 2009. ISBN = 9780470278581.

[13] S. Ergun. Fluid flow through packed columns. *Chemical Engineering Progress*, vol. 48:pp. 89–94, 1952. DOI: http://dx.doi.org/10.1021/ie50474a011, Available at: http://dns2.asia.edu.tw/~ysho/YSHO-English/1000CE/PDF/CheEngPro48,89.pdf.

[14] J. Gan, Z. Zhou, and A. Yu. Particle scale study of heat transfer in packed and fluidized beds of ellipsoidal particles. *Chemical Engineering Science*, vol. 144:pp. 201–215, 2016. DOI = 10.1016/j.ces.2016.01.041, Available at: http://dx.doi.org/10.1016/j.ces.2016.01.041.

[15] Z. Guo, Z. Sun, N. Zhang, M. Ding, H. Bian, and Z. Meng. Computational study on fluid flow and heat transfer characteristic of hollow structured packed bed. *Powder Technology*, vol. 344:pp. 463–474, 2019. DOI = 10.1016/j.powtec.2018.11.101, Available at: https://doi.org/10.1016/j.powtec.2018.11.101.

[16] S. S. Halkarni, A. Sridharan, and S. V. Prabhu. Estimation of volumetric heat transfer coefficient in randomly packed beds of uniform sized spheres with water as working medium. *International Journal of Thermal Sciences*, vol. 110:pp. 340–355, 2016. DOI = 10.1016/j.ijthermalsci.2016.07.012, Available at: http://dx.doi.org/10.1016/j.ijthermalsci.2016.07.012.

[17] S. M. Hasnain. Review on sustainable thermal energy storage technologies, part I: Heat storage materials and techniques. *Energy Conversion and Management*, vol. 39:pp. 1127–1138, 1998. DOI = 10.1016/S0196-8904(98)00025-9, Available at: https://doi.org/10.1016/S0196-8904(98)00025-9.

[18] J. Hliník. *Design optimization of a heat exchanger with a phase change material for thermal energy storage*. Master's thesis, Brno University of Technology, 2017. 70 p., Available at: https://www.vutbr.cz/www_base/zav_prace_soubor_verejne.php?file_id=151334.

[19] K. A. Hoffmann and S. T. Chiang. *Computational fluid dynamics*. Engineering Education System, Wichita, Kansas, 4th edition, 2000. 502 p., ISBN = 0962373109.

[20] W. Hundsdorfer and J. Verwer. *Numerical Solution of Time-Dependent Advection-Diffusion-Reaction Equations in Springer Series in Computational Mathematics*, volume 33. Springer-Verlag, New York, 2003. 471 p., DOI = 10.1007/978-3-662-09017-6, Available at: https://link.springer.com/book/10.1007%2F978-3-662-09017-6.

[21] K. A. Ismail and R. Stuginsky. Parametric study on possible fixed bed models for pcm and sensible heat storage. *Applied Thermal Engineering*, vol. 19:pp. 757–788, 1999. DOI = 10.1016/S1359-4311(98)00081-7, Available at: https://doi.org/10.1016/S1359-4311(98)00081-7.

[22] M. A. Kant, J. Ammann, E. Rossi, C. Madonna, D. Höser, and P. Rudolf von Rohr. Thermal properties of Central Aare granite for temperatures up to 500°C: Irreversible changes due to thermal crack formation. *Geophysical Research Letters*, vol. 44:pp. 771–776, 2017. DOI = 10.1002/2016GL070990, Available at: `https://agupubs.onlinelibrary.wiley.com/doi/pdf/10.1002/2016GL070990`.

[23] G. O. G. Löf and R. W. Hawley. Unsteady-State Heat Transfer between air and loose solids. *Industrial & Engineering Chemistry*, vol. 40:pp. 1061–1070, 1948. DOI = 10.1021/ie50462a017,.

[24] S. Luke. *Essentials of Metaheuristics*. Lulu, 2nd edition, 2013. ISBN = 9781300549628, Available at: `http://cs.gmu.edu/~sean/book/metaheuristics/`.

[25] N. Mphephu. *Numerical Solution of 1-D Convection-Diffusion-Reaction Equation*. Master's thesis, African Institute for Mathematical Sciences, Cape Town, 2013. Available at: `https://www.researchgate.net/publication/258407668_Numerical_Solution_of_1-D_Convection-Diffusion-Reaction_Equation`.

[26] Y. Pinchover and J. Rubinstein. *An Introduction to Partial Differential Equations*. Cambridge University Press, New York, 2005. ISBN = 9780521848862.

[27] S. S. Rao. *Engineering Optimization: Theory and Practice*. John Wiley & Sons, Inc., 4th edition, 2009. DOI= 10.1002/9780470549124.

[28] D. G. Schaeffer and J. W. Cain. *Ordinary Differential Equations: Basics and Beyond*, volume 65. Springer, New york, 2016. DOI = 10.1007/978-1-4939-6389-8, Available at: `http://link.springer.com/10.1007/978-1-4939-6389-8`.

[29] H. Singh, R. P. Saini, and J. S. Saini. A review on packed bed solar energy storage systems. *Renewable and Sustainable Energy Reviews*, 14(3):1059–1069, 2010. DOI = 10.1016/j.rser.2009.10.022, ISSN = 13640321.

[30] H. Singh, R. P. Saini, and J. S. Saini. Performance of a packed bed solar energy storage system having large sized elements with low void fraction. *Solar Energy*, 87(1):22–34, 2013. DOI = 10.1016/j.solener.2012.10.004, ISSN = 0038092X, Available at: `http://dx.doi.org/10.1016/j.solener.2012.10.004`.

[31] A. Singhal, S. Cloete, S. Radl, R. Quinta-Ferreira, and S. Amini. Heat transfer to a gas from densely packed beds of cylindrical particles. *Chemical Engineering Science*, 172:1–12, 2017. DOI = 10.1016/j.ces.2017.06.003, ISBN = 13858947, ISSN = 00092509, Available at: `http://dx.doi.org/10.1016/j.ces.2017.06.003`.

[32] The engineering toolbox: Dry air properties. `https://www.engineeringtoolbox.com`, 2001. Accessed: 2019-03-26.

[33] N. Wakao and S. Kaguei. *Heat and mass transfer in packed bed, Topics in Chemical Engineering*, volume 1. Gordon and Breach Science Publishers, 1982. ISBN = 0-677-05860-8, ISSN = 0277-5883.

[34] S. Whitaker. Forced Convection Heat Transfer Correlations for Flow In Pipes, Past Flat Plates, Single. *AIChE Journal*, 18:361–371, 1972. DOI = 10.1002/aic.690180219, ISBN = 15475905, ISSN = 0001-1541.

[35] G. Zanganeh, A. Pedretti, S. Zavattoni, M. Barbato, and A. Steinfeld. Packed-bed thermal storage for concentrated solar power - Pilot-scale demonstration and industrial-scale design. *Solar Energy*, 86:3084–3098, 2012. DOI = 10.1016/j.solener.2012.07.019, ISSN = 0038092X, Available at: `http://dx.doi.org/10.1016/j.solener.2012.07.019`.

[36] C. Zoppou. *Numerical Solution of the Advective-Diffusion Equation by*. PhD thesis, Australian National University, Canberra, 1994. Available at: `http://hdl.handle.net/1885/114397`.

Used symbols and abbreviations

a	speed of sound [m/s]
a_p	particle superficial area per unit particle volume [m^{-1}]
a_w	superficial area of packed bed per unit packed bed volume [m^{-1}]
A	cross-sectional area [m^2]
A_{int}	area of interest [m^2]
A_p	surface area of particles [m^2]
A_{void}	void area [m^2]
A_t	cross-sectional area of packed bed [m^2]
A_{ins}	cross-sectional of bed with insulation [m^2]
Bi	Biot number [–]
c_f	specific heat of fluid phase [J/kg·K]
c_p	specific heat at constant pressure [J/kg·K]
$c_{p,f}$	specific heat at constant pressure of fluid phase [J/kg·K]
$c_{p,s}$	specific heat at constant pressure of solid phase [J/kg·K]
c_s	specific heat of solid phase [J/kg·K]
c_v	specific heat at constant volume [J/kg·K]
$c_{v,f}$	specific heat at constant volume of fluid phase [J/kg·K]
d_p	particle diameter [m]
d_t	tube diameter [m]
e	insulation thickness [m]
G	superficial mass velocity [kg/s·m^2]
h	heat transfer coefficient [W/m^2·K]
h_p	heat transfer coefficient of particles [W/m^2·K]
h_w	heat transfer coefficient at wall [W/m^2·K]
h_{ins}	heat transfer coefficient between insulation and ambient [W/m^2·K]

k	thermal conductivity [W/m·K]
k_{ef}	total effective thermal conductivity [W/m·K]
$k_{ef,f}$	effective thermal conductivity of fluid phase [W/m·K]
$k_{ef,s}$	effective thermal conductivity of solid phase [W/m·K]
k_f	thermal conductivity of fluid phase [W/m·K]
$k_{f,r}$	thermal conductivity of fluid phase in radial direction [W/m·K]
$k_{f,x}$	thermal conductivity of fluid phase in axial direction [W/m·K]
k_{ins}	thermal conductivity of insulation [W/m·K]
k_s	thermal conductivity of fluid phase [W/m·K]
$k_{s,r}$	thermal conductivity of solid phase in radial direction [W/m·K]
$k_{s,x}$	thermal conductivity of solid phase in axial direction [W/m·K]
L	length of packed bed [m]
L_c	characteristic length [m]
$\dot{m}$	mass flow rate [kg/s]
Ma	Mach number [–]
Ma_c	critical Mach number [–]
Nu	Nusselt number [–]
$\Delta\, p$	pressure drop [Pa]
Pe	Peclet number [–]
Pr	Prandtl number [–]
$\dot{q}$	heat flux [W.m^{-2}]
$\dot{Q}$	heat transfer rate [W]
Q	heat [J]
R	gas constant [J/kg·K]
r	radial position in packed bed [m]
r_p	particle radius [m]
r_t	tube (packed bed) radius [m]

Re	Reynolds number [–]
t	total time [s]
t_0	initial time [s]
T	temperature [K]
T_0	initial temperature of solid phase [K]
$T_{d,f}$, T_1	dimensionless fluid phase temperature [–]
$T_{d,s}$, T_2	dimensionless solid phase temperature [–]
T_f	fluid phase temperature [K]
T_{film}	film temperature [K]
T_i	fluid temperature at the inlet of packed bed [K]
T_o	fluid temperature at the outlet of packed bed [K]
T_s	solid phase temperature [K]
T_{ss}	temperature of a solid surface [K]
T_∞	free flow temperature [K]
U_w	overall heat transfer coefficient between vessel and ambient [W/m^2·K]
v	fluid velocity [m/s]
v_c	critical air velocity [m/s]
v_{sv}	superficial velocity [m/s]
v_∞	free flow velocity [m/s]
V	volume [m^3]
$\dot{V}$	volumetric flow rate [m^3/s]
V_p	particle volume [m^3]
V_t	tube volume [m^3]
V_{void}	void volume [m^3]
x	axial position in packed bed [m]
x_d	dimensionless axial position in packed bed [–]

Greek letters

α	thermal diffusivity [m^2/s]
ε	porosity, void fraction [–]
ρ	density [kg/m^3]
ρ_f	density of fluid phase [kg/m^3]
ρ_s	density of solid phase [kg/m^3]
μ	dynamic viscosity [kg/m·s]
ν	kinematic viscosity [m^2/s]
γ	Poisson ratio [–]
λ	ratio of volumetric thermal capacities [–]
Γ	Stanton number for particle [–]
Γ_w	Stanton number at wall [–]
τ	dimensionless time [–]
ψ	sphericity [–]

Abbreviations

ADRE	advection-diffusion-reaction equation
BC	boundary condition
CSPM	continuous solid phase model
FDM	finite difference method
HTF	heat transfer fluid
HSU	heat storage unit
IC	initial condition
NFDM	nonstandard finite difference method
PB	packed bed
PDE	partial differential equation
SFDM	standard finite difference method
TES	thermal energy storage

Subscripts

0	initial
c	critical
d	dimensionless
ef	effective
f	fluid phase
film	evaluating properties at film temperature
i	inlet
ins	insulation
int	item or property of interest
o	outlet
p	particle
r	radial direction
s	solid phase
ss	solid surface
t	internal tube of packed bed
void	considering empty space in PB
w	wall
∞	ambient